

Supplementary Information

Simple Photocleavable Indoline-based Materials for Surface Wettability Patterning

Alex S. Loch^a, Douglas Cameron^b, Robert W. Martin^b, Peter J. Skabara^a and Dave J. Adams^{a*}

^a *School of Chemistry, University of Glasgow, G12 8QQ, U.K.*; ^b *Department of Physics, SUPA, University of Strathclyde, G4 0NG, U.K.*

* Corresponding author, E-mail address: dave.adams@glasgow.ac.uk

Contact Angle Measurements after Thermal Annealing

Table S1: Static contact angle measurements after heating and before, and after 365 nm LED irradiation. The results are an average of a minimum of 4 measurements on a single film, with the given error as the standard deviation. Changes of $<10^\circ$ are not shown. For heating above each materials T_g : **6-*t*Bu** and **10-*t*Bu** were heated at 75°C , **7-OH** was heated at 90°C , **8-*t*Bu** and **9-OH** were heated at 55°C , and **11-OH** was heated at 105°C for 5 mins before being allowed to cool to room temperature and tested. For heating above each materials melting point: **6-*t*Bu** and **8-*t*Bu** were heated at 180°C , **7-OH**, **9-OH**, and **10-*t*Bu** were heated at 195°C , and **11-OH** was heated at 280°C for 5 min before being allowed to cool to room temperature and tested.

($^\circ$)	After T_g	After UV	Change	After MP	After UV	Change
6-<i>t</i>Bu	81 ± 2	72 ± 1	-	62 ± 2	59 ± 1	-
7-OH	53 ± 2	80 ± 2	27	61 ± 1	65 ± 2	-
8-<i>t</i>Bu	45 ± 1	54 ± 1	-	67 ± 3	61 ± 1	-
9-OH	34 ± 2	72 ± 1	38	65 ± 1	65 ± 3	-
10-<i>t</i>Bu	72 ± 2	71 ± 1	-	78 ± 2	72 ± 1	-
11-OH	81 ± 1	82 ± 1	-	66 ± 1	61 ± 1	-

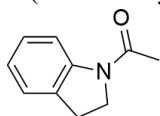
Materials and Methods

General Experimental

Anhydrous dichloromethane was dried on an Innovative Technology PS-400 solvent purification system. Anhydrous pyridine was dried by standing over 3 \AA molecular sieves before being decanted for use. Thin layer chromatography (TLC) was performed using aluminium backed silica gel 60 F_{254} plates. Column chromatography was performed using Merck silica gel, 60 \AA 230–400 mesh. Where solvent mixtures are used, the proportions are given by volume. ^1H and ^{13}C NMR spectra were recorded on a Bruker Avance^{III} 400 MHz spectrometer. Chemical shifts (δ) are reported in parts per million (ppm) to the residual solvent peak (CDCl_3 : 7.26 ppm for ^1H and 77.0 ppm for ^{13}C ; $\text{DMSO-}d_6$: 2.50 ppm for ^1H and 39.52 ppm for ^{13}C). Coupling constants (J) are given to the nearest 0.1 Hertz (Hz). Peak multiplicities are reported as singlet (s), doublet (d), triplet (t), multiplet (m), or broad (b). Peak assignments are reported as: H_{Ar} = aromatic H or C_{Ar} = aromatic C. High resolution accurate mass measurements (HRMS) were performed on an Agilent 6546 LC/QTOF (quadrupole-time of flight) instrument with an Agilent ESI or APCI source. Infrared absorption spectra were recorded on an Agilent Cary 630 FTIR spectrometer as neat samples using an ATR attachment. Differential scanning calorimetry (DSC) was performed on a Netzsch DSC 214 Polyma. Thermal gravimetric analysis (TGA) was carried out on a Netzsch TG 209 Tarsus and are corrected for the crucible. Melting points (mp) were measured in a glass capillary using a Stuart SMP50 automatic melting point apparatus and are uncorrected. Solutions used for film fabrication were prepared by dissolving the sample in tetrahydrofuran at a concentration of 10 mg/mL or 15 mg/mL. For neat film fabrication, polished fused silica (12 mm diameter, 2 mm thickness) or microscope slide pieces ($15 \times 15 \text{ mm}$, 1.5 mm thickness) were used as the substrates and were cleaned by washing with acetone and 2-propanol before being blow dry under a stream of compressed air. Films were prepared by covering the cleaned substrates with the stock solution before spinning on a Cookson electronics SCS G3-8 spin coater with a spin speed of 2000 RPM and a spin time of 60 s. Films were dried in a vacuum oven at 40°C for a minimum for 1 h or as discussed. Absorption spectra were measured on an Agilent Cary 60 UV–vis spectrophotometer either dissolved in UV-grade tetrahydrofuran or as the neat film. NMR studies to investigate photocleavage were completed at a concentration of 7 mg/mL. Microscope images were taken on a Nikon Eclipse LV100ND with a $5\times$ magnification using transmitted and polarised light. For the static contact angle measurements, a 2 μL droplet (automatic pipette) of deionised water was lowered until it contacted the surface. As soon as the droplet was transferred from the pipette tip to the surface the tip was retracted, and the static contact angle measured after 1 s (in all cases) to allow for droplet stabilisation. Visualisation of the droplet and automated angle calculation was completed using an Ossila Contact Angle Goniometer using Ossila Contact Angle software. Atomic force microscopy (AFM) studies were conducted on a Bruker Dimension FastScan using a RFESP-75 tip.

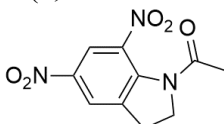
Material Synthesis

1-(Indolin-1-yl)ethan-1-one (**2**)



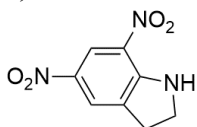
2 was prepared following an established procedure¹ (14.1 g, 94%); mp: 103 °C. Note: pronounced effects of restricted rotation were observed in the ¹H NMR resulting in each signal being split. ¹H NMR (400 MHz, CDCl₃) δ: 8.21 (0.8H, d, *J* 8.0, H_{Ar}), 7.25–7.10 (2.3H, m, H_{Ar}), 7.01 (0.9H, td, *J* 7.4, 1.2, H_{Ar}), 4.14 (0.5H, bt, *J* 8.2, N-CH₂), 4.05 (1.5H, t, *J* 8.5, N-CH₂), 3.20 (1.7H, t, *J* 8.5, N-CH₂-CH₂), 3.06 (0.3H, bt, *J* 7.7, N-CH₂-CH₂), 2.44 (0.5H, s, CH₃), 2.23 (2.5H, s, CH₃). ¹³C NMR (101 MHz, CDCl₃) δ: 168.8 (C=O), 143.0 (C_{Ar}), 131.2 (C_{Ar}), 127.6 (CH_{Ar}), 124.6 (CH_{Ar}), 123.7 (CH_{Ar}), 117.1 (CH_{Ar}), 48.9 (N-CH₂), 28.1 (N-CH₂-CH₂), 24.3 (CH₃). HRMS (ESI/QTOF) *m/z*: [M+H]⁺ calcd for C₁₀H₁₂NO 162.0913 (100%), 163.0945 (11%); found 162.0917 (100%), 163.0947 (12%).

1-(5,7-Dinitroindolin-1-yl)ethan-1-one (**3**)



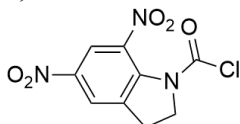
3 was prepared following an established procedure¹ (2.21 g, 94%); mp: 209 °C (decomposition). ¹H NMR (400 MHz, DMSO-*d*₆) δ: 8.45–8.40 (2H, m, H_{Ar}), 4.36 (2H, t, *J* 8.3, N-CH₂), 3.32 (2H, t, *J* 7.8, N-CH₂-CH₂), 2.26 (3H, s, CH₃). ¹³C NMR (101 MHz, DMSO-*d*₆) δ: 169.3 (C=O), 142.6 (C_{Ar}), 139.9 (C_{Ar}), 139.2 (C_{Ar}), 138.2 (C_{Ar}), 123.6 (CH_{Ar}), 119.1 (CH_{Ar}), 50.5 (N-CH₂), 28.0 (N-CH₂-CH₂), 23.3 (CH₃). HRMS (APCI/QTOF) *m/z*: [M-H]⁻ calcd for C₁₀H₈N₃O₅ 250.0469 (100%), 251.0498 (12%); found 250.0470 (100%), 251.0498 (11%).

5,7-Dinitroindoline (**4**)



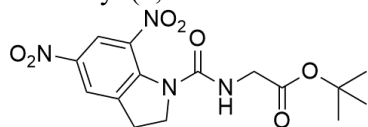
4 was prepared following an established procedure¹ (1.20 g, 96%); mp: 242 °C. UV-vis: λ_{max} (tetrahydrofuran)/nm 263 (log ε/dm³ mol⁻¹ cm⁻¹, 3.93), 362 (4.09), 389sh (3.84). ¹H NMR (400 MHz, CDCl₃) δ: 8.85 (1H, d, *J* 2.0, H_{Ar}), 8.02 (1H, s, H_{Ar}), 7.34 (1H, bs, NH), 4.06 (2H, t, *J* 8.7, N-CH₂), 3.31 (2H, t, *J* 8.7, N-CH₂-CH₂). ¹³C NMR (101 MHz, CDCl₃) δ: 151.6 (C_{Ar}), 137.4 (C_{Ar}), 135.6 (C_{Ar}), 125.3 (C_{Ar}), 122.5 (CH_{Ar}), 121.1 (CH_{Ar}), 47.7 (N-CH₂), 26.6 (N-CH₂-CH₂). HRMS (ESI/QTOF) *m/z*: [M+H]⁺ calcd for C₈H₈N₃O₄ 210.0509 (100%), 211.0536 (10%); found 210.0511 (100%), 211.0545 (10%).

5,7-Dinitroindoline-1-carbonyl chloride (**5**)



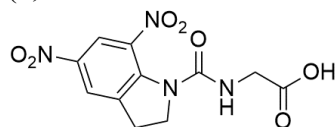
Intermediate **5** was prepared as required following an established procedure¹ and was used in subsequent reactions without purification. ¹H NMR was used to confirm complete conversion to the acyl chloride. ¹H NMR (400 MHz, CDCl₃) δ: 8.62 (1H, d, *J* 2.0, H_{Ar}), 8.32 (1H, dt, *J* 2.3, 1.3, H_{Ar}), 4.61 (2H, t, *J* 8.0, N-CH₂), 3.41 (2H, t, *J* 8.3, N-CH₂-CH₂).

tert-Butyl (5,7-dinitroindoline-1-carbonyl)glycinate (**6-*t*Bu**)



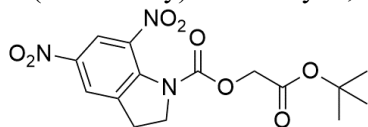
A mixture of **5** (5.32 g, \approx 19.6 mmol), glycine *tert*-butyl ester hydrochloride (3.16 g, 18.9 mmol), and *N,N*-dimethylpyridin-4-amine (5.10 g, 41.7 mmol) in anhydrous dichloromethane (40 mL) was stirred overnight under nitrogen. The solution was then diluted with dichloromethane (20 mL) and hydrochloric acid (aq. 1M, 40 mL). The layers were separated, and the aqueous layer was extracted with dichloromethane (2×40 mL). The combined organic extracts were washed with water (2×100 mL), dried over anhydrous sodium sulfate, filtered, and the solvent removed to give a yellow solid. The solid was initially purified by column chromatography over silica using dichloromethane as the eluent to afford the crude product as a light-yellow solid. The solid was sonicated in diethyl ether (20 mL), and collected at the filter to give **6-*t*Bu** as a bright yellow solid (3.29 g, 48%); mp: 178 °C; mp (DSC): 174 °C (onset first heating cycle, 10 °C min⁻¹). IR (solid) ν /cm⁻¹: 1748 (C=O), 1739 (C=O). UV-vis: λ_{max} (tetrahydrofuran)/nm 260sh (log ϵ /dm³ mol⁻¹ cm⁻¹, 3.67), 355 (4.13). ¹H NMR (400 MHz, CDCl₃) δ : 8.60 (1H, d, *J* 2.2, H_{Ar}), 8.20 (1H, dt, *J* 2.2, 1.3, H_{Ar}), 5.41 (1H, bt, *J* 4.5, NH), 4.35 (2H, t, *J* 8.2, N-CH₂), 4.00 (2H, d, *J* 4.9, NH-CH₂), 3.39 (2H, ddt, *J* 9.5, 8.3, 1.1, N-CH₂-CH₂), 1.49 (9H, s, CH₃). ¹³C NMR (101 MHz, CDCl₃) δ : 169.2 (C=O-O), 154.3 (N-C=O), 142.3 (C_{Ar}), 142.1 (C_{Ar}), 137.6 (C_{Ar}), 137.1 (C_{Ar}), 123.2 (CH_{Ar}), 120.5 (CH_{Ar}), 83.2 (C-CH₃), 51.1 (N-CH₂), 43.3 (NH-CH₂), 28.4 (N-CH₂-CH₂), 28.2 (CH₃). HRMS (ESI/QTOF) *m/z*: [M+Na]⁺ calcd for C₁₅H₁₈N₄NaO₇ 389.1068 (100%), 390.1097 (18%); found 389.1077 (100%), 390.1106 (18%). *T_d*: (5% weight loss) 190 °C. *T_g* (DSC): 61 °C (second scan, 50 °C min⁻¹).

(5,7-Dinitroindoline-1-carbonyl)glycine (**7-OH**)



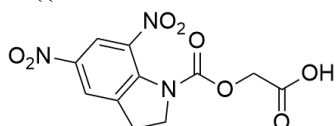
A solution of **6-*t*Bu** (1.15 g, 3.14 mmol) in dichloromethane (50 mL) and trifluoroacetic acid (30 mL) was stirred in the dark for 1 h. The solvent and excess trifluoroacetic acid was removed to give a yellow solid. The solid was sonicated in chloroform (10 mL) and collected at the filter to give the cde product. The solid was further purified by stirring in a diethyl ether:tetrahydrofuran mixture (1:10), was collected at the filter, and dried to give **7-OH** as a light yellow solid (937 mg, 96%); mp: 190 °C (decomposition); mp (DSC): 185 °C (onset first heating cycle, 10 °C min⁻¹). IR (solid) ν /cm⁻¹: 3321 (OH), 1732 (C=O). UV-vis: λ_{max} (tetrahydrofuran)/nm 261sh (log ϵ /dm³ mol⁻¹ cm⁻¹, 3.67), 354 (4.12). ¹H NMR (400 MHz, DMSO-*d*₆) δ : 12.65 (1H, bs, COOH), 8.41 (1H, d, *J* 2.4, H_{Ar}), 8.33 (1H, d, *J* 2.4, H_{Ar}), 8.02 (1H, t, *J* 6.0, NH), 4.26 (2H, t, *J* 8.8, N-CH₂), 3.79 (2H, d, *J* 5.9, N-CH₂), 3.35 (2H, t, *J* 8.8, N-CH₂-CH₂). ¹³C NMR (101 MHz, DMSO-*d*₆) δ : 171.1 (C=OOH), 154.7 (C=O-NH), 142.1 (C_{Ar}), 140.9 (C_{Ar}), 138.5 (C_{Ar}), 136.3 (C_{Ar}), 123.3 (CH_{Ar}), 119.5 (CH_{Ar}), 51.3 (N-CH₂), 41.8 (NH-CH₂), 27.6 (N-CH₂-CH₂). HRMS (ESI/APCI) *m/z*: [M+H]⁺ calcd for C₁₁H₁₁N₄O₇ 311.0622 (100%), 312.0650 (14%); found 311.06213 (100%), 312.0654 (14%). *T_d*: (5% weight loss) 199 °C. *T_g* (DSC): 86 °C.

2-(*tert*-Butoxy)-2-oxoethyl 5,7-dinitroindoline-1-carboxylate (**8-*t*Bu**)



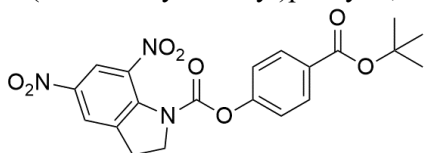
A mixture of **5** (2.60 g, ≈ 9.57 mmol), *tert*-butyl 2-hydroxyacetate (1.15 g, 8.70 mmol), and *N,N*-dimethylpyridin-4-amine (2.20 g, 18.0 mmol) in anhydrous dichloromethane (40 mL) was stirred overnight under nitrogen. The solution was then diluted with dichloromethane (20 mL) and hydrochloric acid (aq. 1M, 20 mL). The layers were separated, and the aqueous layer was extracted with dichloromethane (2×30 mL). The combined organic extracts were washed with water (2×50 mL), dried over anhydrous sodium sulfate, filtered on a silica plug that was washed with dichloromethane (50 mL), and the solvent removed to give the crude product as a yellow solid. The solid was sonicated in a diethyl ether:*n*-hexane mixture (1:3) and collected at the filter to give **8-*t*Bu** as a yellow solid (2.97 g, 93%); mp 151 °C; mp (DSC): 146 °C (onset first peak, first heating cycle, 10 °C min⁻¹), 177 °C (onset second peak, first heating cycle, 10 °C min⁻¹). IR (solid) ν/cm^{-1} : 1720 (C=O). UV-vis: λ_{max} (tetrahydrofuran)/nm 258sh (log $\epsilon/\text{dm}^3 \text{ mol}^{-1} \text{ cm}^{-1}$, 3.70), 338 (4.04). ¹H NMR (400 MHz, CDCl₃) δ : 8.58 (1H, d, *J* 2.3, H_{Ar}), 8.24 (1H, d, *J* 2.3, H_{Ar}), 4.62 (2H, s, O-CH₂), 4.45 (2H, t, *J* 8.2, N-CH₂), 3.35 (2H, t, *J* 8.5, N-CH₂-CH₂), 1.47 (9H, s, CH₃). ¹³C NMR (101 MHz, CDCl₃) δ : 166.5 (CH₂-C=O), 152.3 (N-C=O), 143.3 (C_{Ar}), 140.4 (C_{Ar}), 138.5 (C_{Ar}), 138.3 (C_{Ar}), 123.3 (CH_{Ar}), 120.2 (CH_{Ar}), 83.2 (C-CH₃), 63.0 (O-CH₂), 50.8 (N-CH₂), 28.2 (N-CH₂-CH₂ or CH₃), 28.1 (N-CH₂-CH₂ or CH₃). HRMS (ESI/QTOF) *m/z*: [M+NH₄]⁺ calcd for C₁₅H₂₁N₄O₈ 385.1354 (100%), 386.1383 (18%); found 385.1356 (100%), 386.1390 (20%). *T*_d: (5% weight loss) 186 °C. *T*_g (DSC): 45 °C (second scan, 50 °C min⁻¹).

2-((5,7-Dinitroindoline-1-carbonyl)oxy)acetic acid (**9-OH**)



A solution of **8-*t*Bu** (1.81 g, 4.93 mmol) in dichloromethane (50 mL) and trifluoroacetic acid (30 mL) was stirred for 1 h. The solvent and excess trifluoroacetic acid was removed to give a yellow solid. The solid was sonicated in chloroform (50 mL), collected at the filter, and dried to give **9-OH** as a light-yellow solid (1.22 g, 80%); mp 187 °C; mp (DSC): 188 °C (onset first heating cycle, 10 °C min⁻¹). IR (solid) ν/cm^{-1} : 1724 (C=O). UV-vis: λ_{max} (tetrahydrofuran)/nm 258sh (log $\epsilon/\text{dm}^3 \text{ mol}^{-1} \text{ cm}^{-1}$, 3.70), 338 (4.04). UV-vis: λ_{max} (tetrahydrofuran)/nm 258sh (log $\epsilon/\text{dm}^3 \text{ mol}^{-1} \text{ cm}^{-1}$, 3.69), 338 (4.05). ¹H NMR (400 MHz, DMSO-*d*₆) δ : 13.24 (1H, bs, COOH), 8.49 (1H, d, *J* 1.4, H_{Ar}), 8.43 (1H, d, *J* 1.4, H_{Ar}), 4.69 (2H, s, O-CH₂), 4.34 (2H, t, *J* 8.5, N-CH₂), 3.35 (2H, t, *J* 8.5, N-CH₂-CH₂). ¹³C NMR (101 MHz, DMSO-*d*₆) δ : 168.7 (COOH), 152.3 (N-C=O), 142.7 (C_{Ar}), 139.7 (C_{Ar}), 139.5 (C_{Ar}), 137.3 (C_{Ar}), 123.8 (CH_{Ar}), 119.6 (CH_{Ar}), 62.5 (O-CH₂), 50.7 (N-CH₂), 27.7 (N-CH₂-CH₂). HRMS (APCI/QTOF) *m/z*: [2M-H]⁻ calcd for C₂₂H₁₇N₆O₁₆ 621.0707 (100%), 622.0735 (27%); found 621.0708 (100%), 622.0738 (27%). *T*_d: (5% weight loss) 223 °C. *T*_g (DSC): 46 °C (second scan, 50 °C min⁻¹).

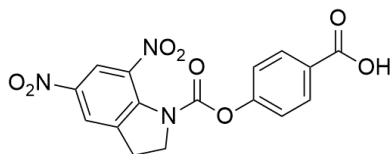
4-(*tert*-Butoxycarbonyl)phenyl 5,7-dinitroindoline-1-carboxylate (**10-*t*Bu**)



A mixture of **5** (2.60 g, ≈ 9.57 mmol), *tert*-butyl 4-hydroxybenzoate (1.70 g, 8.71 mmol), and *N,N*-dimethylpyridin-4-amine (2.20 g, 18.0 mmol) in anhydrous dichloromethane (40 mL) was stirred overnight under nitrogen. The solution was then diluted with hydrochloric acid (aq. 1M, 30 mL) and the layers were separated. The organic layer was washed with water (2×50 mL), dried over anhydrous sodium sulfate, filtered, and the solvent removed to give a yellow solid. The solid was initially purified by column chromatography over silica using dichloromethane as the eluent to afford the crude product

as a light-yellow solid. The solid was then sonicated in diethyl ether (30 mL), collected at the filter, and dried to give **10-tBu** as a yellow solid (2.47 g, 66%); mp 188 °C; mp (DSC): 189 °C (onset first heating cycle, 10 °C min⁻¹). IR (solid) ν/cm^{-1} : 1754 (C=O). UV-vis: λ_{max} (tetrahydrofuran)/nm 259sh (log $\epsilon/\text{dm}^3 \text{ mol}^{-1} \text{ cm}^{-1}$, 3.90), 337 (4.06). ¹H NMR (400 MHz, CDCl₃) δ : 8.60 (1H, d, *J* 2.2, H_{Ar1}), 8.29 (1H, d, *J* 2.2, H_{Ar1}), 8.02 (2H, d, *J* 8.8, H_{Ar}), 7.21 (2H, d, *J* 8.4, H_{Ar}), 4.53 (2H, t, *J* 8.4, N-CH₂), 3.40 (2H, t, *J* 8.4, N-CH₂-CH₂), 1.59 (9H, s, CH₃). ¹³C NMR (101 MHz, CDCl₃) δ : 164.9 (C_{Ar}-C=O), 153.3 (C_{Ar}-O), 150.5 (N-C=O), 143.7 (C_{Ar}), 139.9 (C_{Ar}), 138.62 (C_{Ar}), 138.56 (C_{Ar}), 131.3 (CH_{Ar}), 130.4 (C_{Ar}), 123.6 (CH_{Ar1}), 121.1 (CH_{Ar}), 120.4 (CH_{Ar1}), 81.5 (C-CH₃), 51.2 (N-CH₂), 28.3 (CH₃). 28.2 (N-CH₂-CH₂). HRMS (ESI/APCI) *m/z*: [M+NH₄]⁺ calcd for C₂₀H₂₃N₄O₈ 447.1510 (100%), 448.1540 (24%); found 447.1507 (100%), 448.1537 (24%). *T_d*: (5% weight loss) 219 °C. *T_g* (DSC): 67 °C (second scan, 50 °C min⁻¹).

4-((5,7-Dinitroindoline-1-carbonyl)oxy)benzoic acid (**11-OH**)



A solution of **10-tBu** (1.03 g, 2.40 mmol) in dichloromethane (50 mL) and trifluoroacetic acid (30 mL) was stirred for 1 h. The solvent and excess trifluoroacetic acid was removed to give a coloured solid. The solid was sonicated in chloroform (50 mL), collected at the filter, and dried to give **11-OH** as an off white solid (860 mg, 96%); mp 278 °C (decomposition). IR (solid) ν/cm^{-1} : 1745 (C=O). UV-vis: λ_{max} (tetrahydrofuran)/nm 232 (log $\epsilon/\text{dm}^3 \text{ mol}^{-1} \text{ cm}^{-1}$, 4.46), 259sh (3.93), 336 (4.05). ¹H NMR (400 MHz, DMSO-*d*₆) δ : 13.08 (1H, bs, COOH), 8.53 (1H, d, *J* 2.3, H_{Ar}), 8.50–8.48 (1H, m, H_{Ar}), 8.02 (2H, d, *J* 8.7, H_{Ar}), 7.35 (2H, d, *J* 8.8, H_{Ar}), 4.49 (2H, t, *J* 8.0, N-CH₂), 3.41 (2H, t, *J* 7.8, N-CH₂-CH₂). ¹³C NMR (101 MHz, DMSO-*d*₆) δ : 166.5 (COOH), 153.4 (C_{Ar}-O), 150.6 (C=O), 143.0 (C_{Ar}), 140.1 (C_{Ar}), 139.5 (C_{Ar}), 137.5 (C_{Ar}), 131.5 (C_{Ar}), 131.0 (CH_{Ar}), 128.7 (C_{Ar}), 124.0 (CH_{Ar}), 121.7 (CH_{Ar}), 119.6 (CH_{Ar}), 51.2 (N-CH₂), 27.8 (N-CH₂-CH₂). HRMS (ESI/APCI) *m/z*: [M+H]⁺ calcd for C₁₆H₁₂N₃O₈ 374.0619 (100%), 375.0649 (19%); found 374.0618 (100%), 375.0649 (19%). *T_d*: (5% weight loss) 309 °C. *T_g* (DSC): 96 °C (second scan, 50 °C min⁻¹).

Supplementary Figures

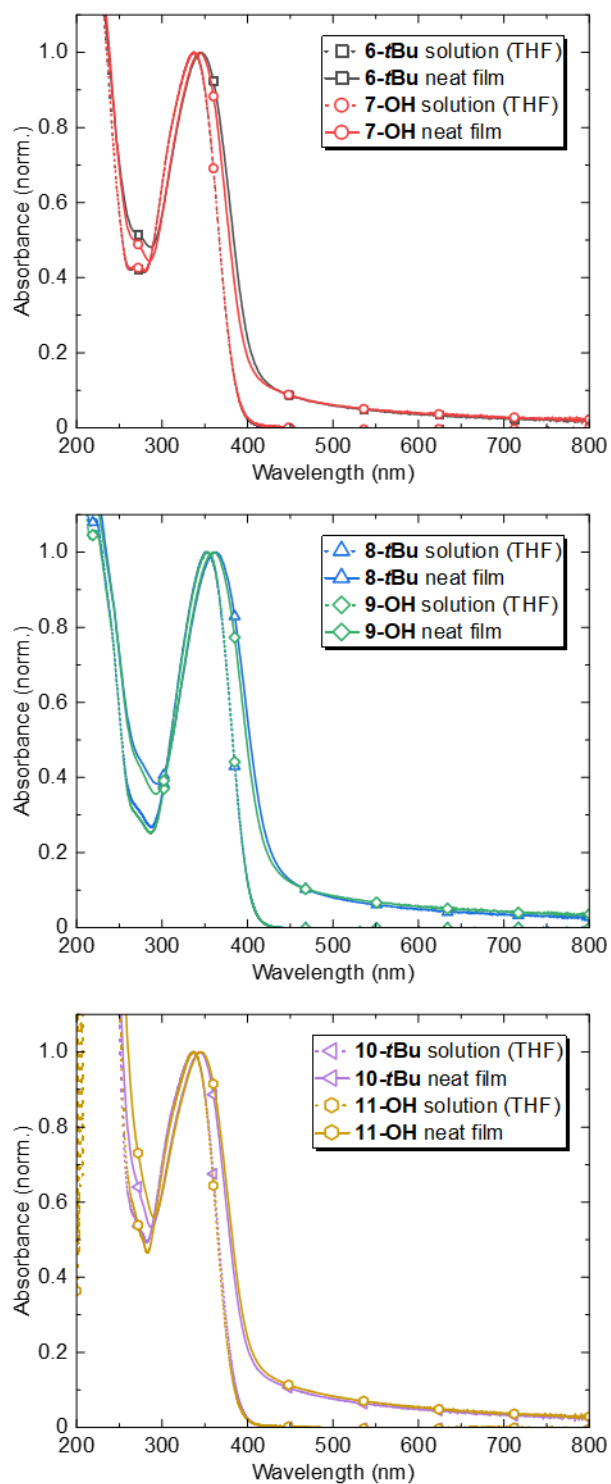


Figure S1: Solution (dashed lines) and film (solid lines) UV-vis absorption for each of the materials.

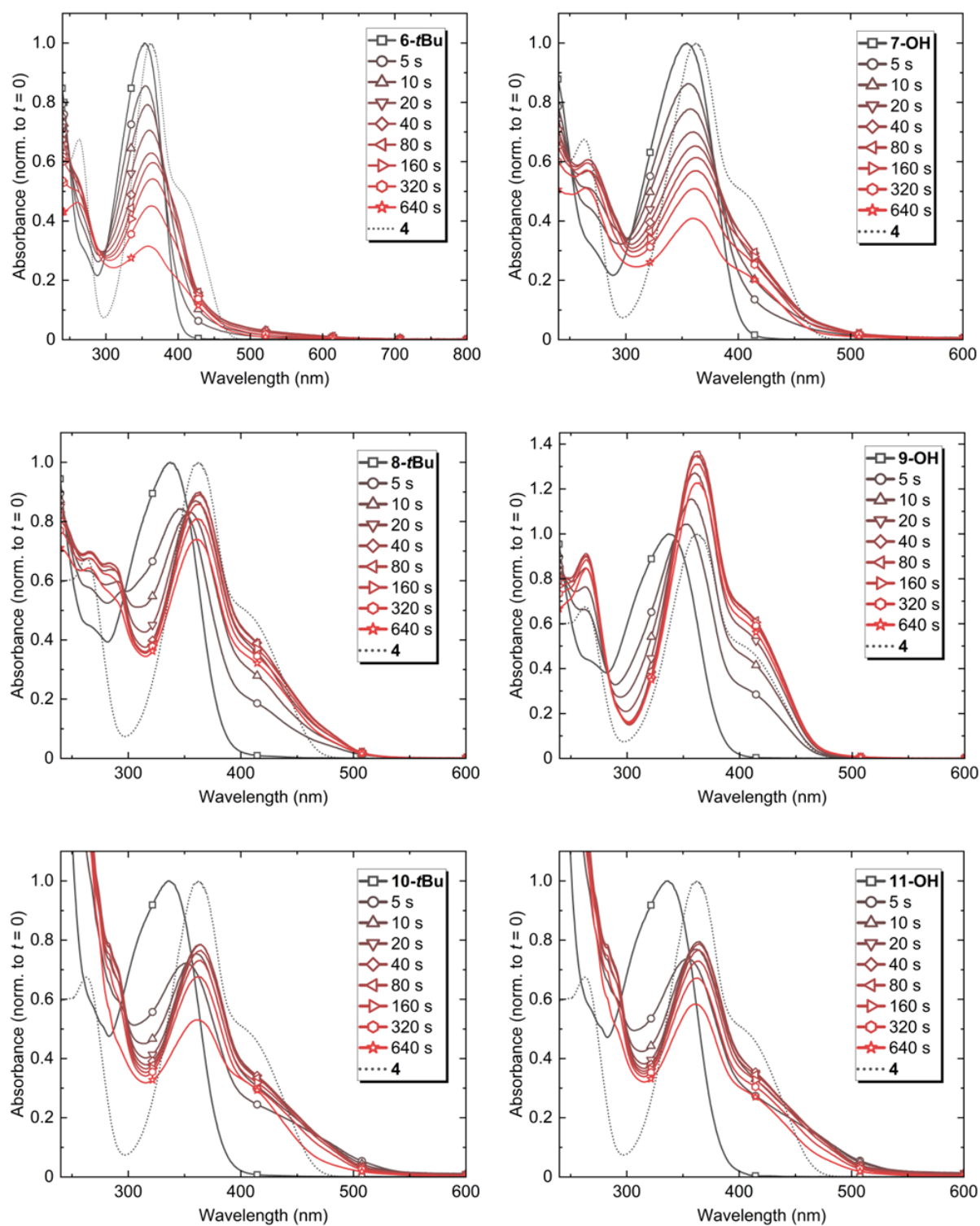


Figure S2: Partial UV-vis spectrum of each of the materials in tetrahydrofuran solution before and after 365 nm LED irradiation, overlaid with the proposed photoproduct, 4. The irradiation power was 161 mW/cm².

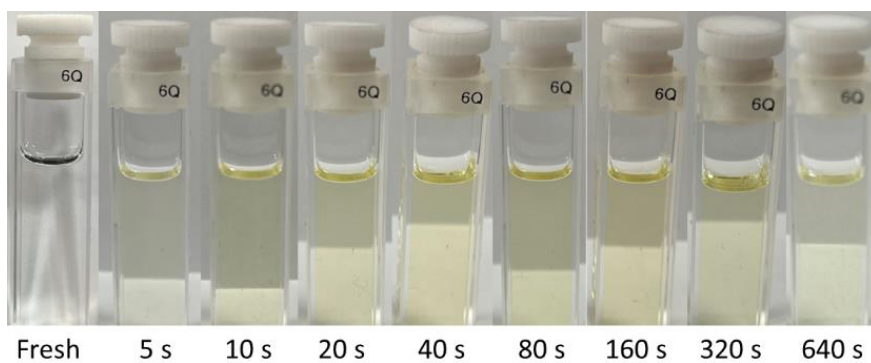


Figure S3: Photographs of 7-OH in tetrahydrofuran before and after 365 nm LED irradiation. The irradiation power was 161 mW/cm².

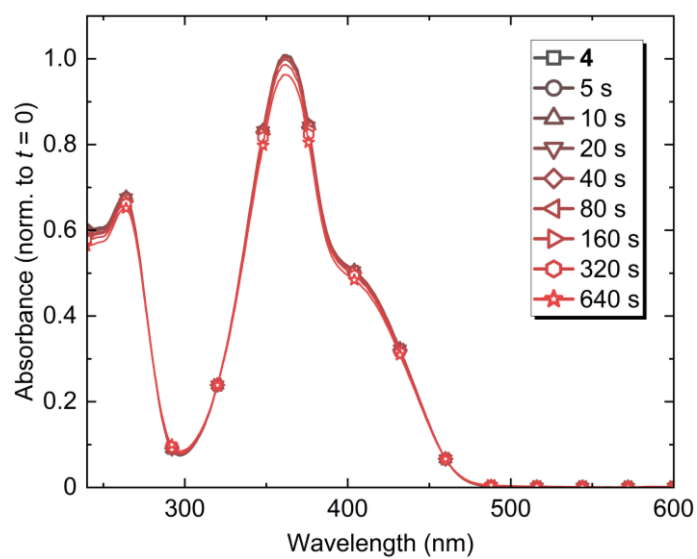


Figure S4: Partial UV-vis spectrum of 4 in tetrahydrofuran solution before and after 365 nm LED irradiation. The slight decrease in the peak absorbance at 320 and 640 s is attributed to photodegradation. The irradiation power was 161 mW/cm².

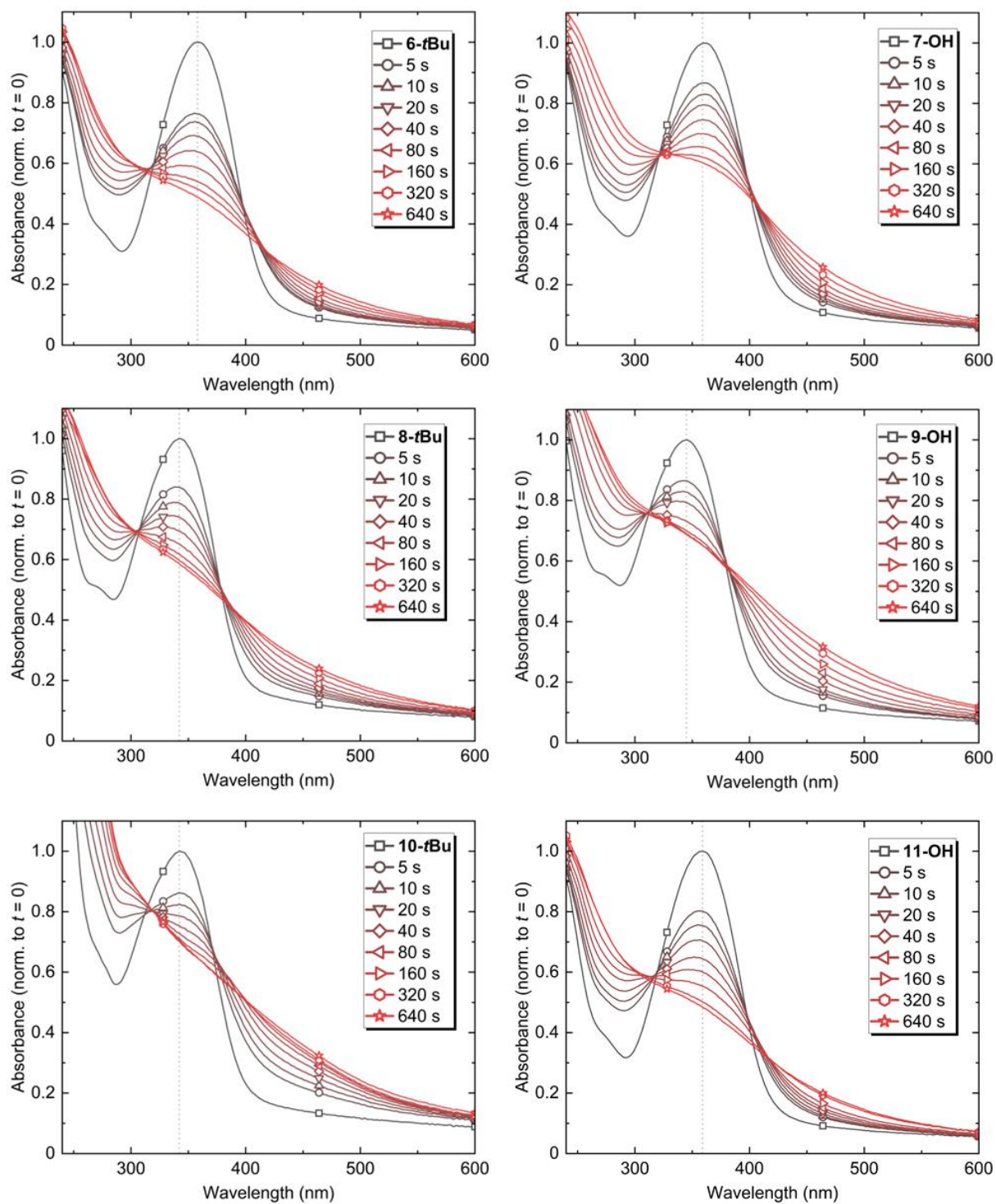


Figure S5: Partial neat film UV-vis spectrum of each of the materials before and after 365 nm LED irradiation. The irradiation power was 161 mW/cm². The dashed vertical line represents the absorption change plotted in **Figure 3c**.

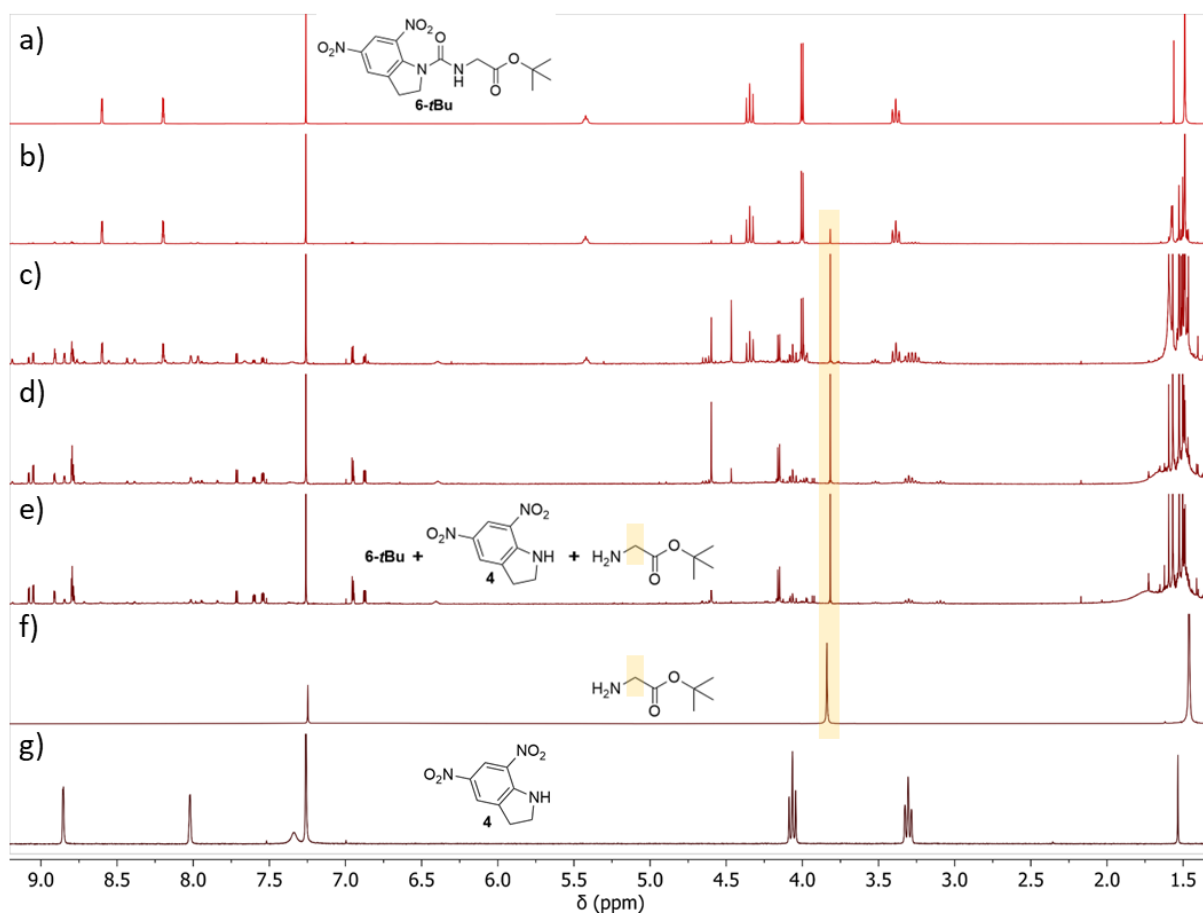


Figure S6: Partial ^1H NMR (400 MHz, CDCl_3) spectra of a-e) **6-tBu** after 0, 1, 5, 15, and 30 mins irradiation by 2×365 nm LEDs (161 mW/cm^2 each); f) *tert*-butyl glycinate; and g) **4**. The shaded areas across the spectra highlight the change in some key signal peaks indicating photocleavage to the proposed photoproducts.

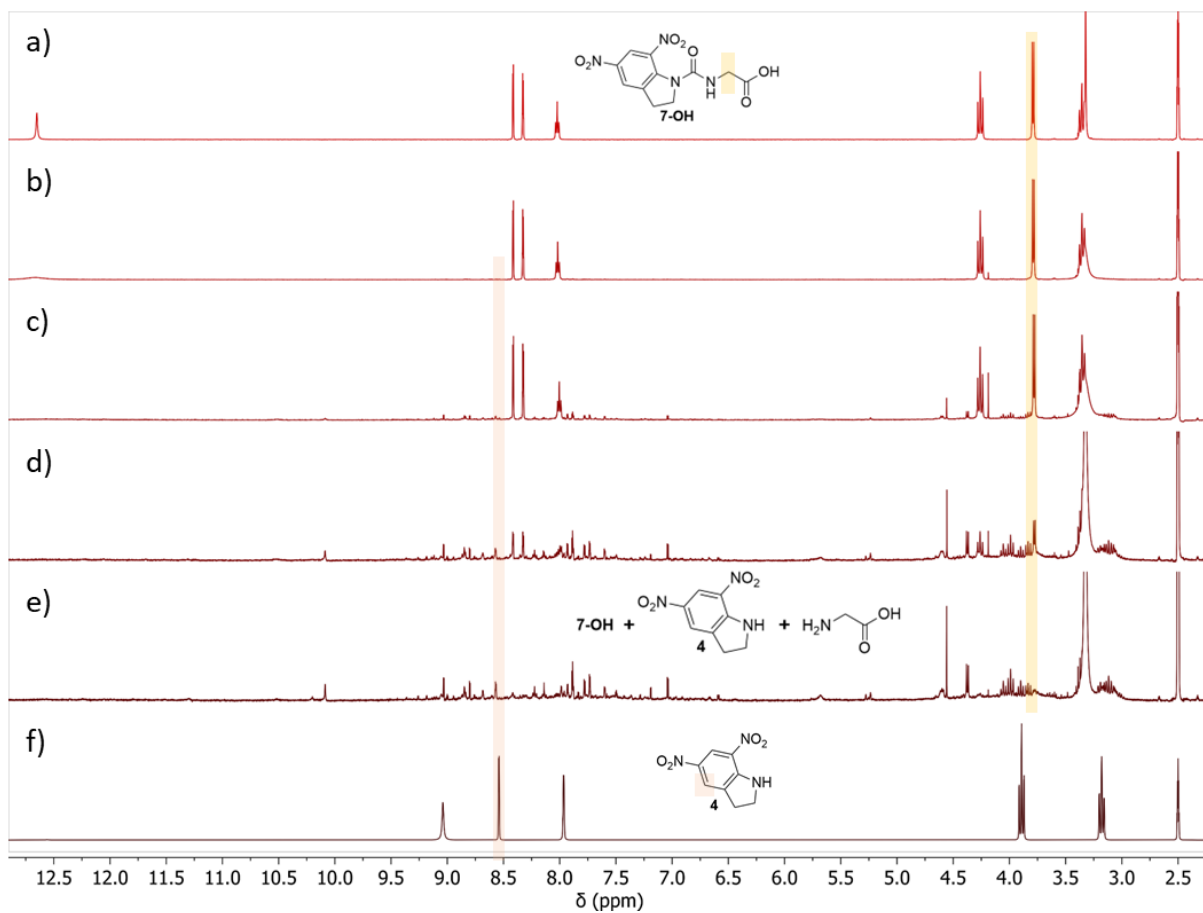


Figure S7: Partial ^1H NMR (400 MHz, DMSO-d_6) spectra of a-e) **7-OH** after 0, 1, 5, 15, and 30 mins irradiation by 2×365 nm LEDs (161 mW/cm^2 each); and f) **4**. The shaded areas across the spectra highlight the change in some key signal peaks indicating photocleavage to the proposed photoproducts.

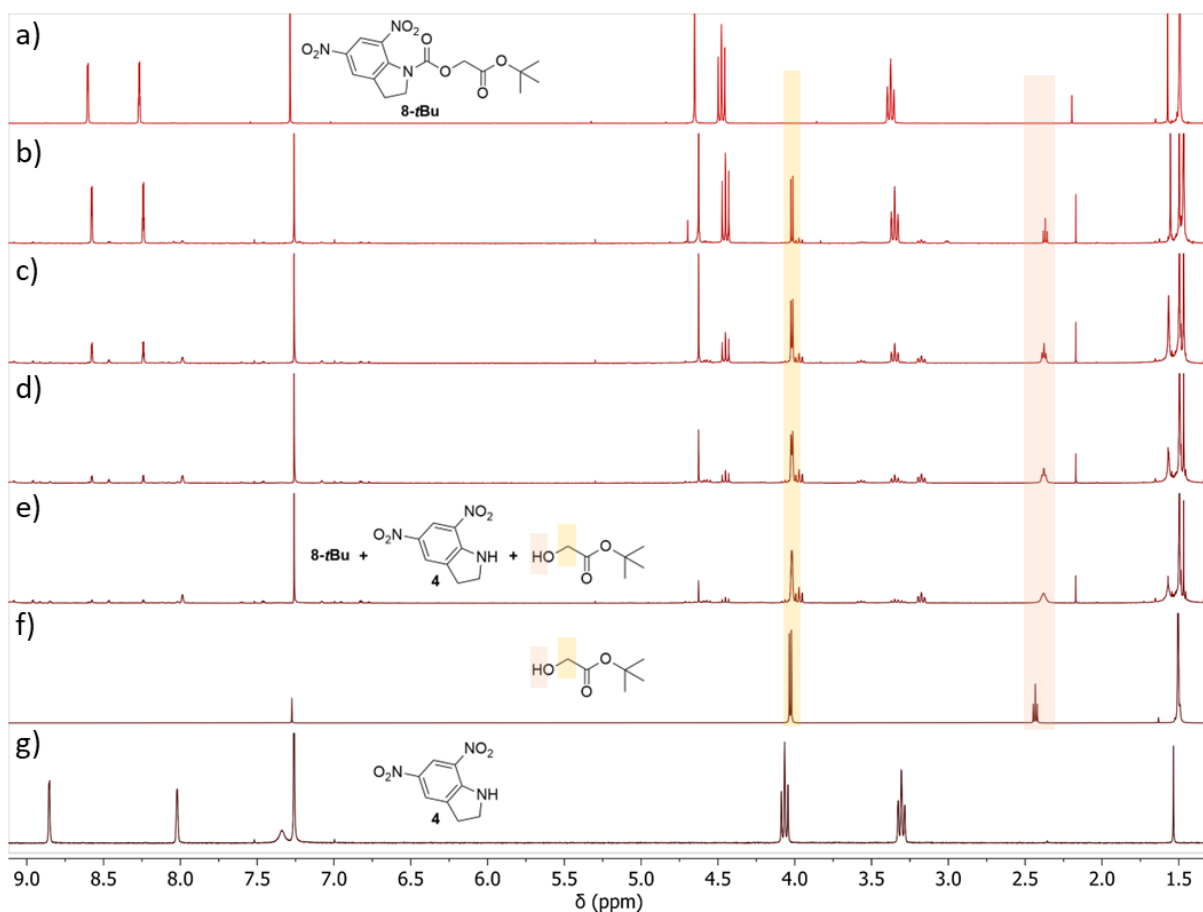


Figure S8: Partial ^1H NMR (400 MHz, CDCl_3) spectra of a-e) **8-tBu** after 0, 1, 5, 15, and 30 mins irradiation by 2×365 nm LEDs (161 mW/cm^2 each); f) *tert*-butyl 2-hydroxyacetate; and g) **4**. The shaded areas across the spectra highlight the change in some key signal peaks indicating photocleavage to the proposed photoproducts.

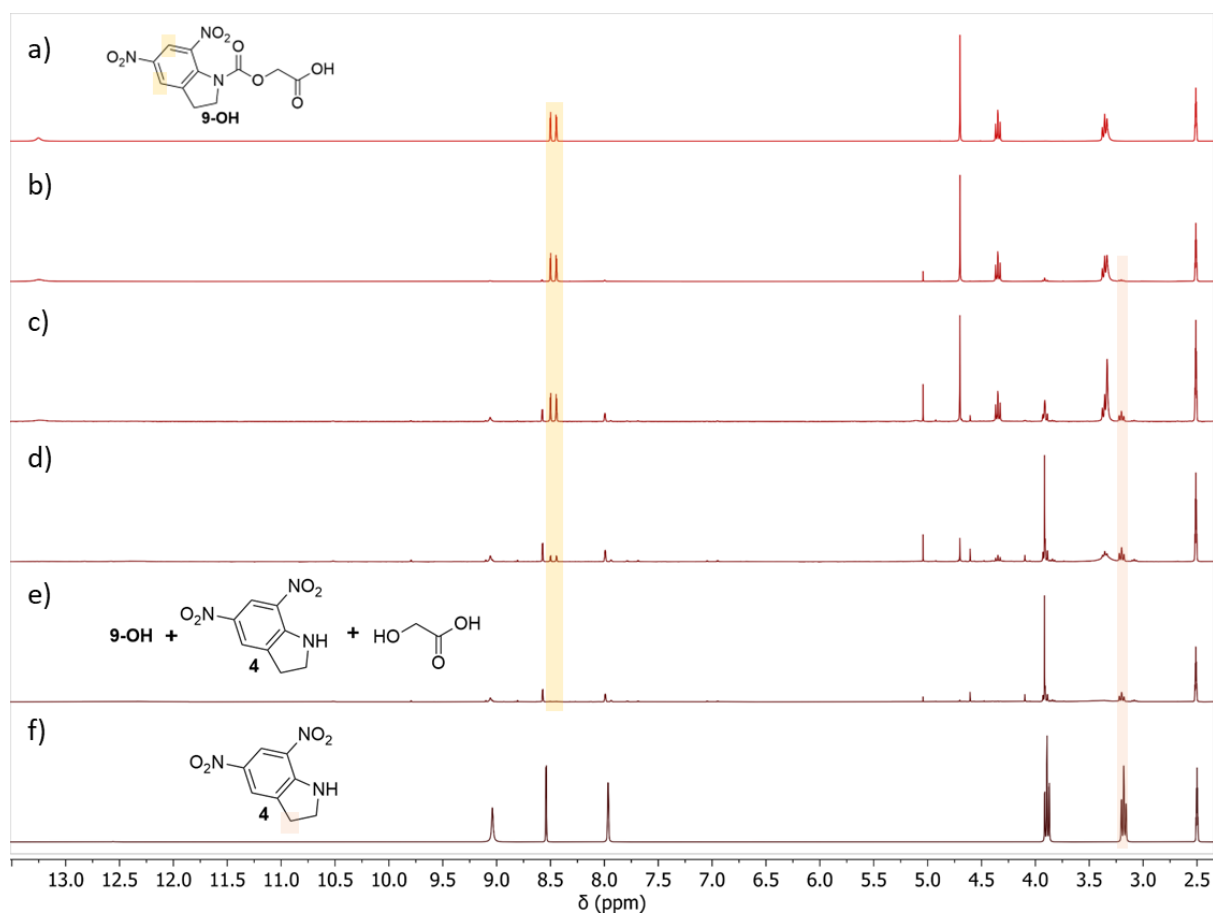


Figure S9: Partial ^1H NMR (400 MHz, DMSO-d_6) spectra of a-e) **9-OH** after 0, 1, 5, 15, and 30 mins irradiation by 2×365 nm LEDs (161 mW/cm^2 each); and f) **4**. The shaded areas across the spectra highlight the change in some key signal peaks indicating photocleavage to the proposed photoproducts.

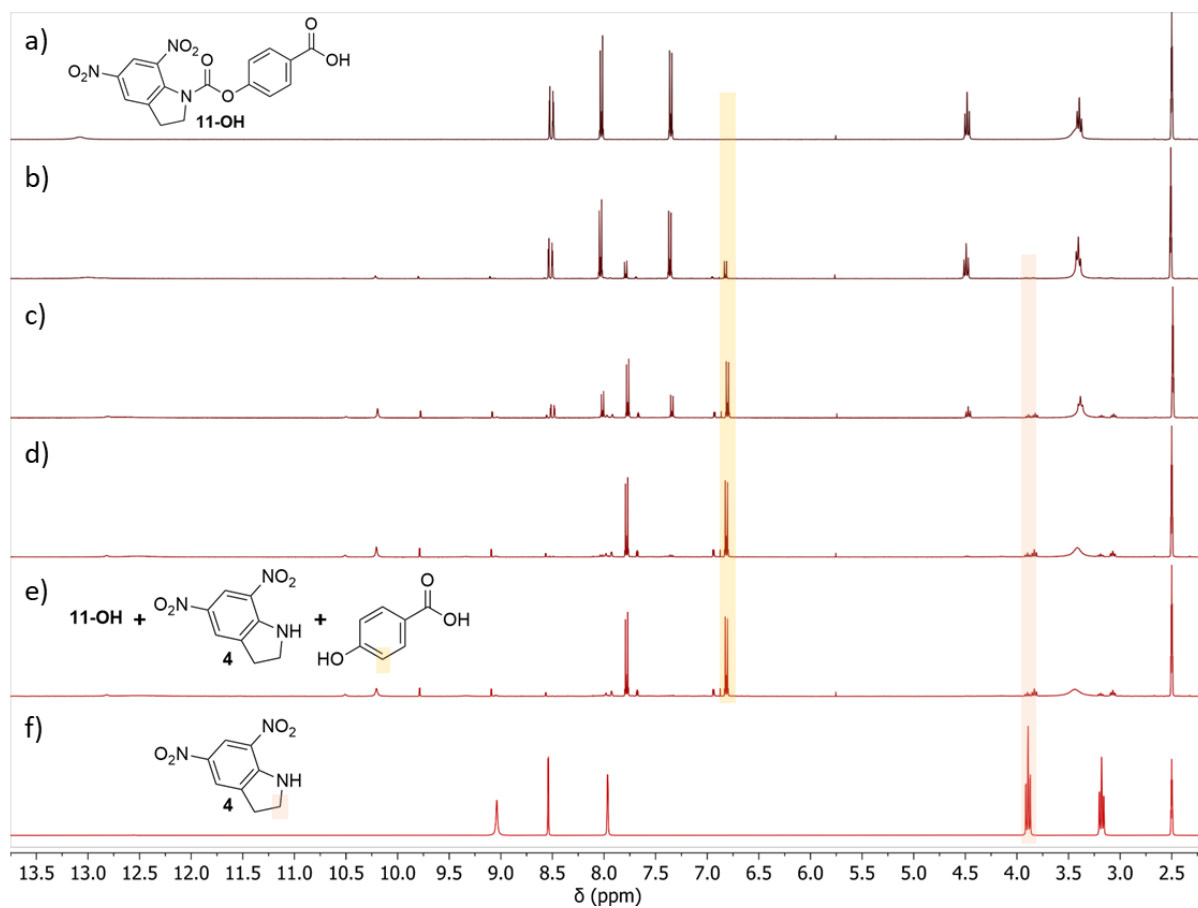


Figure S10: Partial ^1H NMR (400 MHz, DMSO-d_6) spectra of a-e) **11-OH** after 0, 1, 5, 15, and 30 mins irradiation by 2×365 nm LEDs (161 mW/cm^2 each); and f) **4**. The shaded areas across the spectra highlight the change in some key signal peaks indicating photocleavage to the proposed photoproducts.

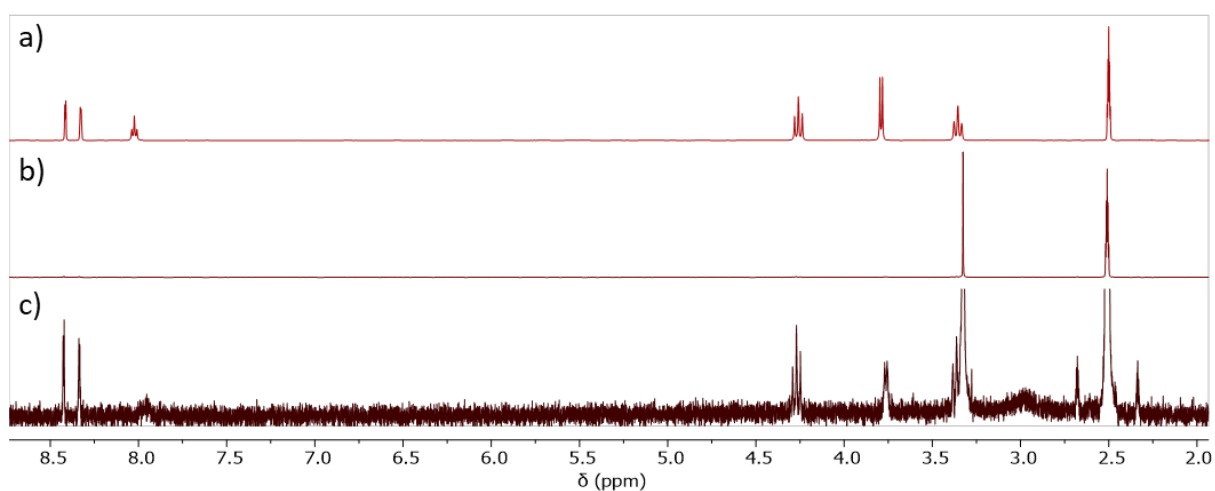


Figure S11: Partial ^1H NMR (400 MHz, DMSO-d_6) spectra of a) **7-OH**; b) a thick film of **7-OH** and c) zoomed view of b).

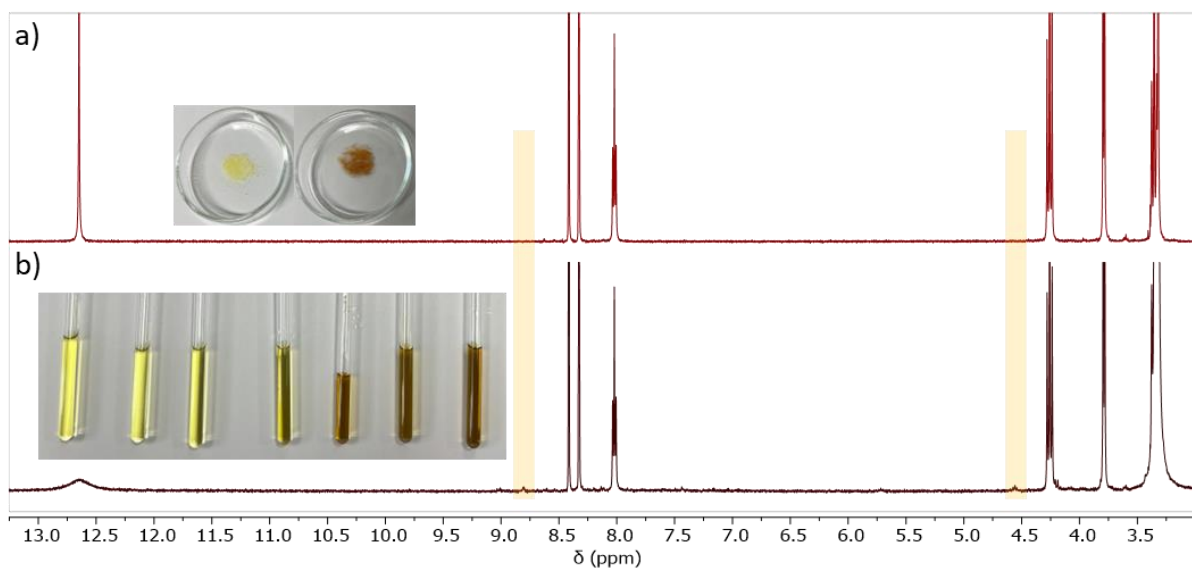


Figure S12: Partial ^1H NMR (400 MHz, DMSO-d_6) spectra of a) **7-OH** (insert left: picture of **7-OH**; insert right: picture of **7-OH** after 4 h irradiation); and b) **7-OH** after 4 h irradiation by 2×365 nm LEDs at 270 mW/cm^2 each (insert from left to right: picture of the NMR tube sample with **7-OH** after 0, 1, 5, 10, 30, 60, and 240 min irradiation). The shaded area across both spectra shows the suspected peak signal arising from the proposed photoproducts.

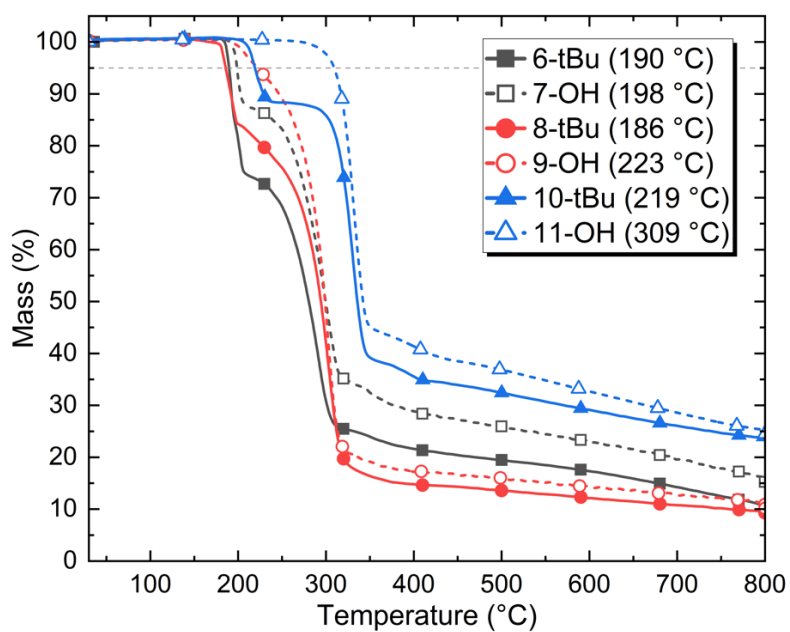


Figure S13: TGA thermographs for each of the materials. The dashed horizontal line represents a 5% mass loss (T_d).

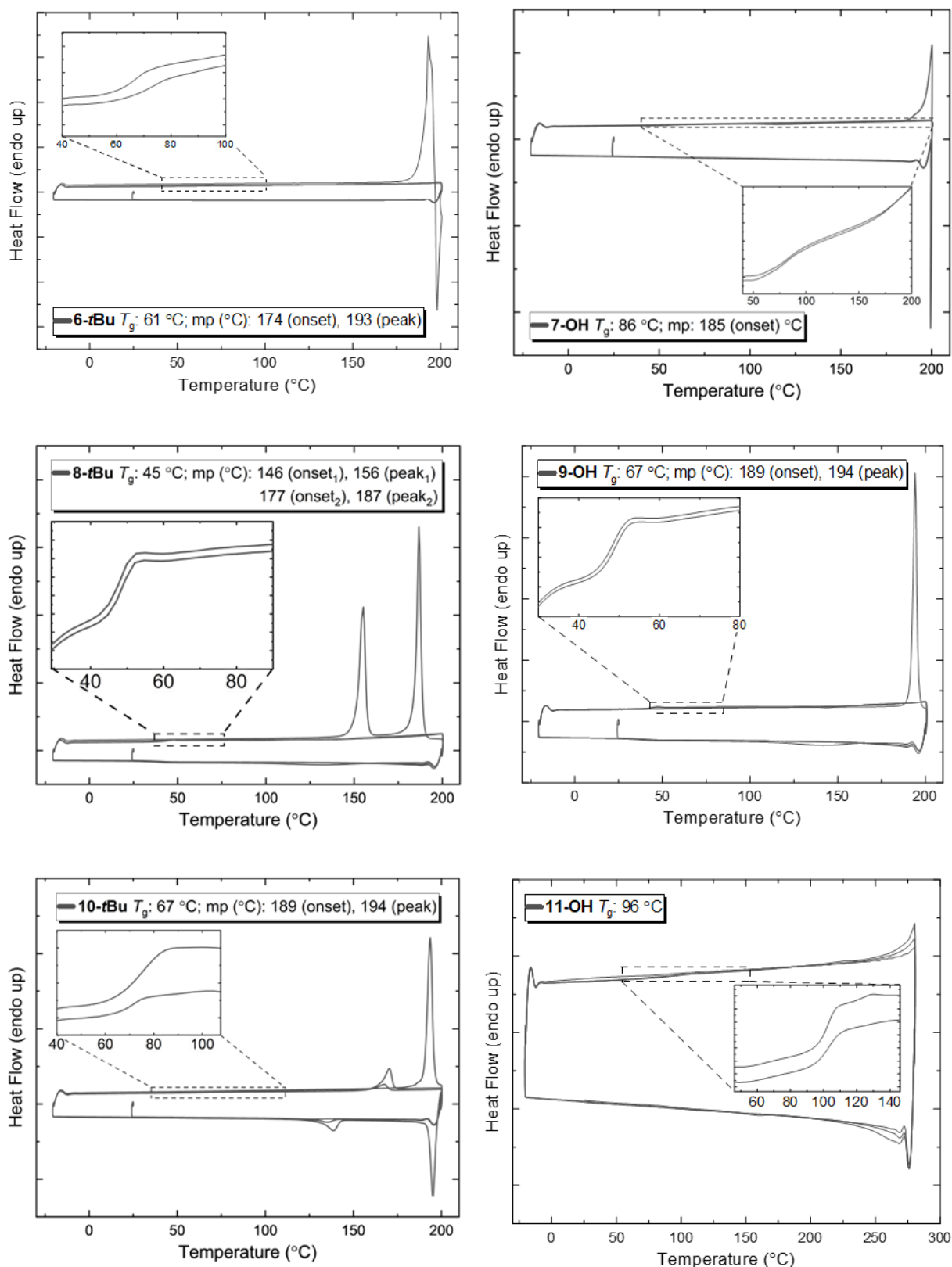


Figure S14: DSC thermograms for each of the materials run at 10 °C/min for three cycles. The insert in each shows a zoomed section with a glass transition feature (T_g), run at 50 °C/min, with the first cycle removed for clarity.

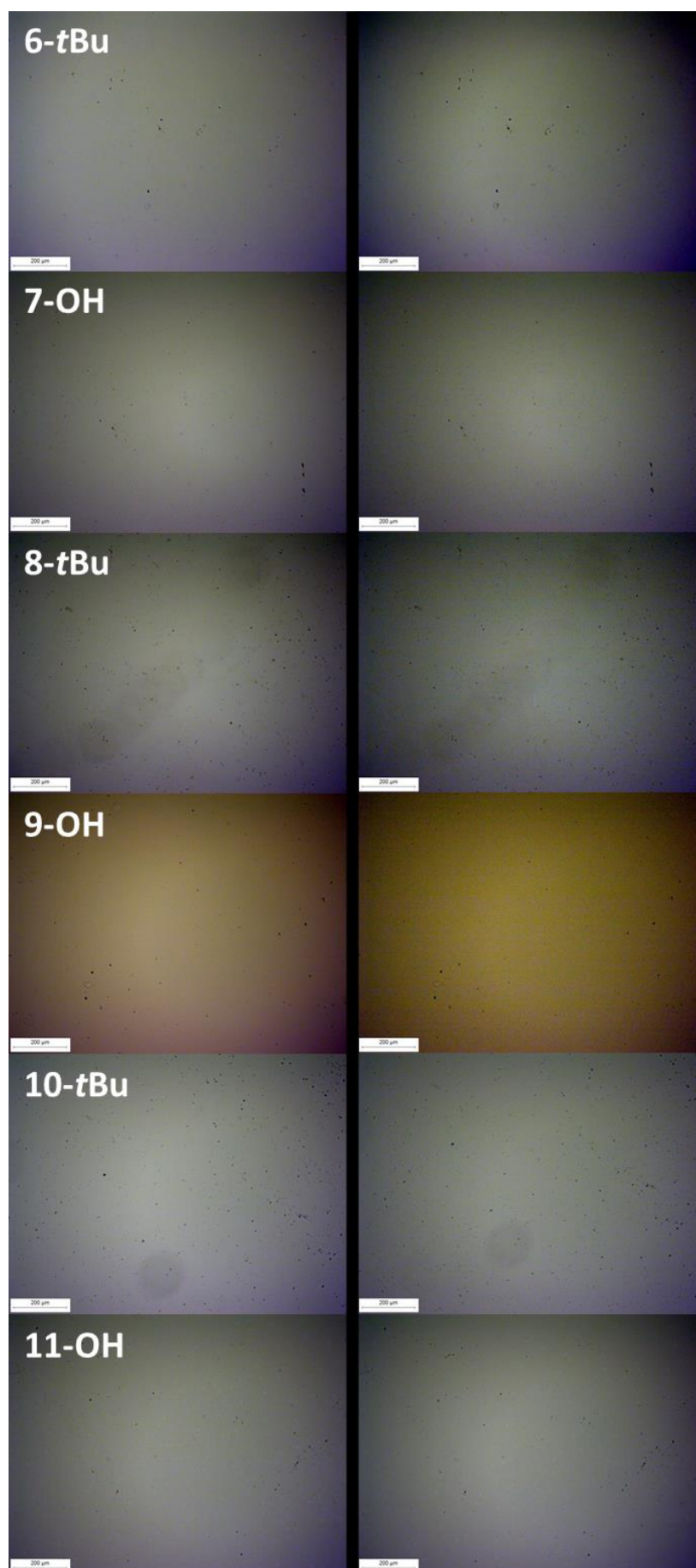


Figure S15: Optical (left) and cross-polarised (right) microscopy images of neat, thin films of each of the materials.

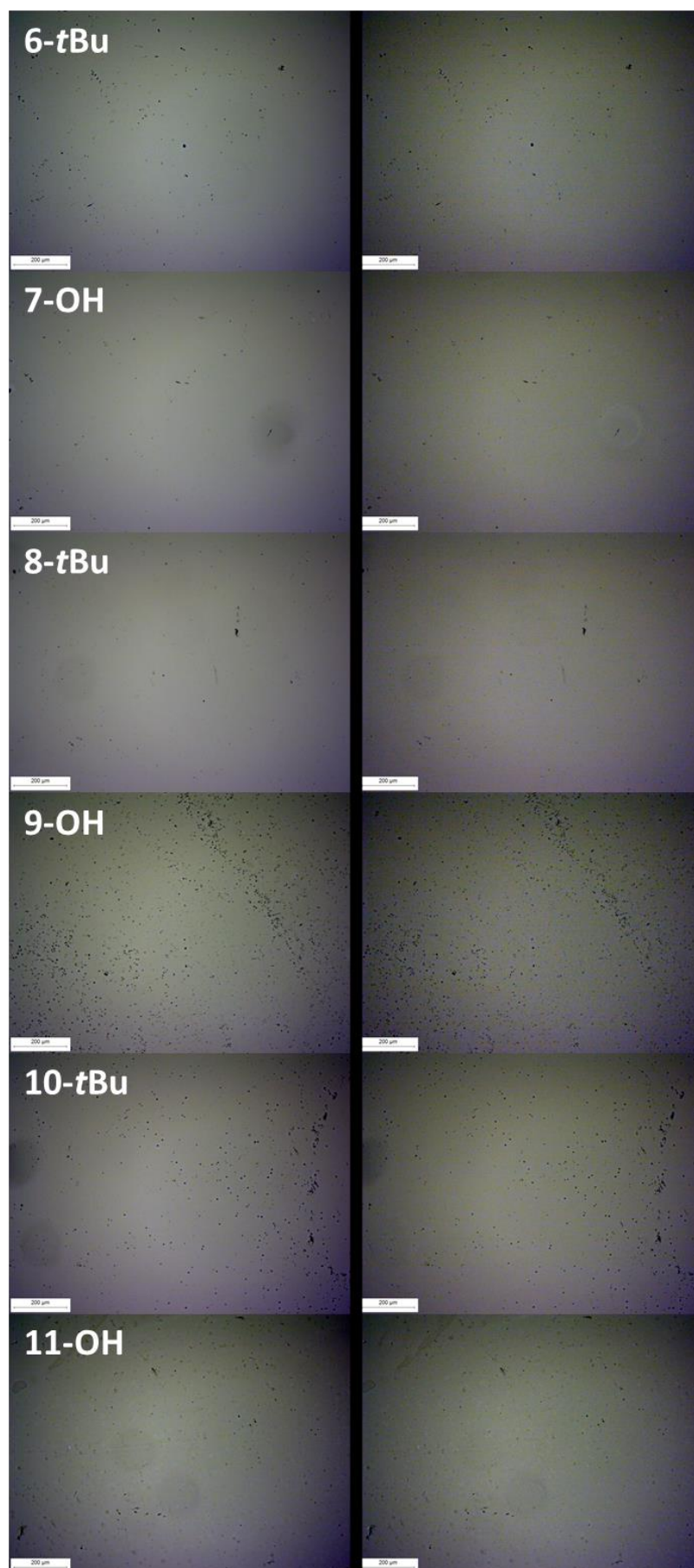


Figure S16: Optical (left) and cross-polarised (right) microscopy images of neat, thin films of each of the materials after 365 nm LED irradiation (161 mW/cm², 5 min).

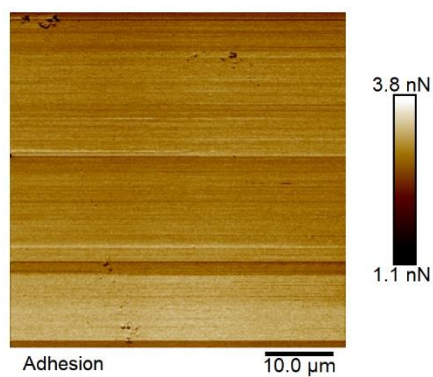


Figure S17: Adhesion map of the small area scan of **7-OH** (Figure 7a). Note: horizontal stripes in the adhesion map are due to lose material attaching to the AFM tip (dust), slightly changing the sample-tip interaction between each pass.

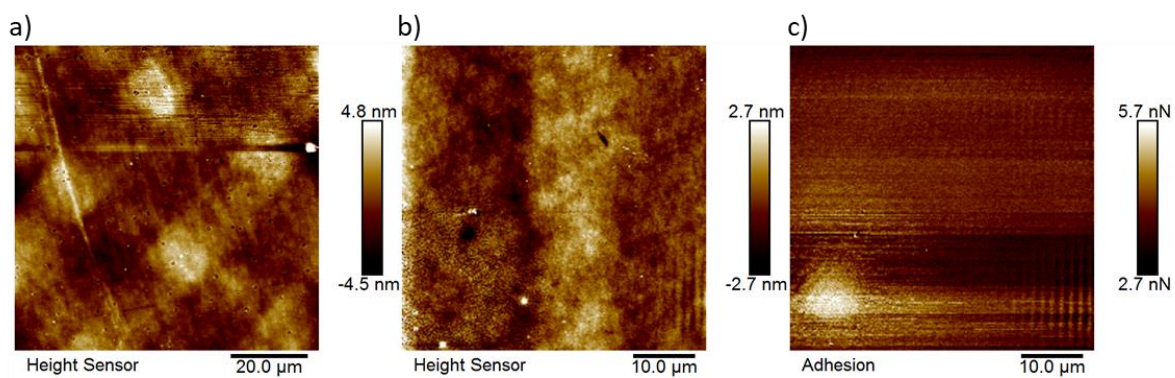


Figure S18: a) AFM height map of a dual, perpendicular grid pattern exposure of a neat, thin film of **9-OH**. Smaller area AFM b) height map and c) adhesion map of a photopatterned neat, thin film of **9-OH**.

¹H, ¹³C, and 2D NMR Spectra

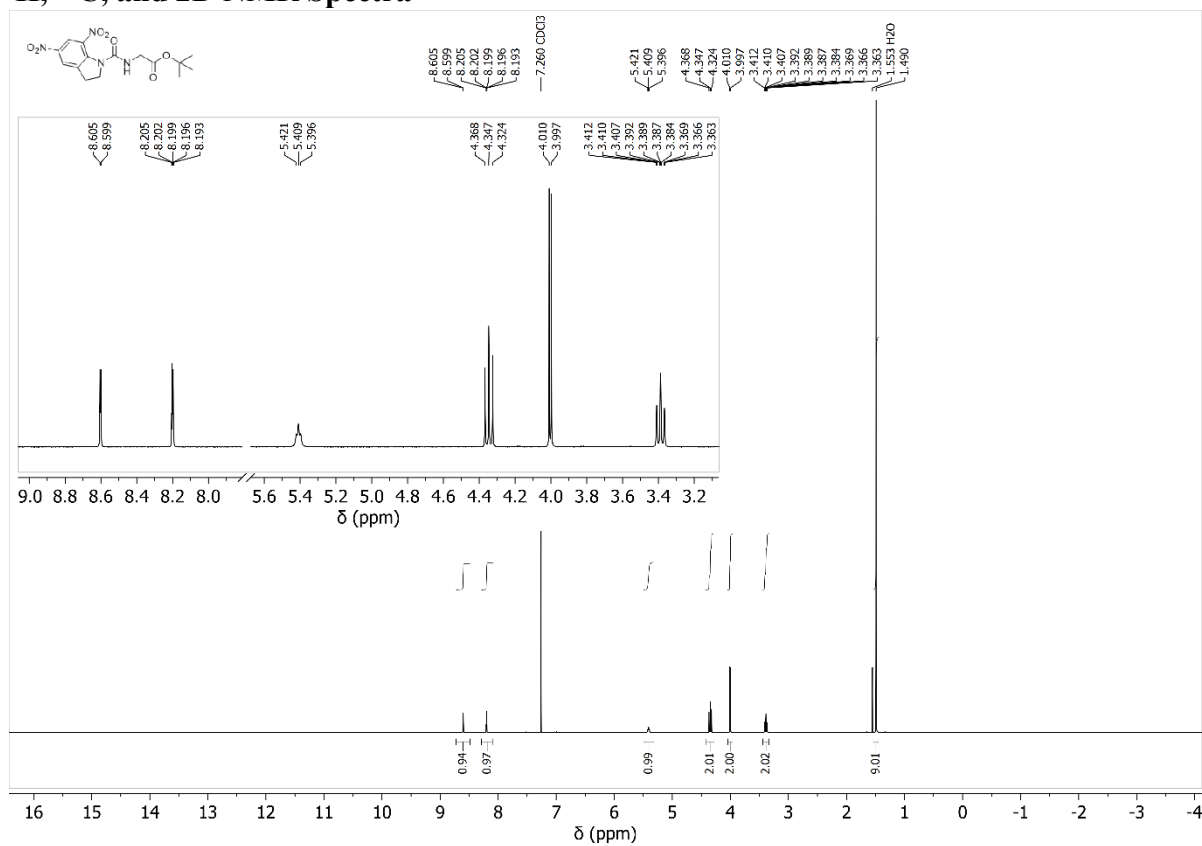


Figure S19: ¹H NMR (400 MHz, CDCl₃) spectra of 6-tBu.

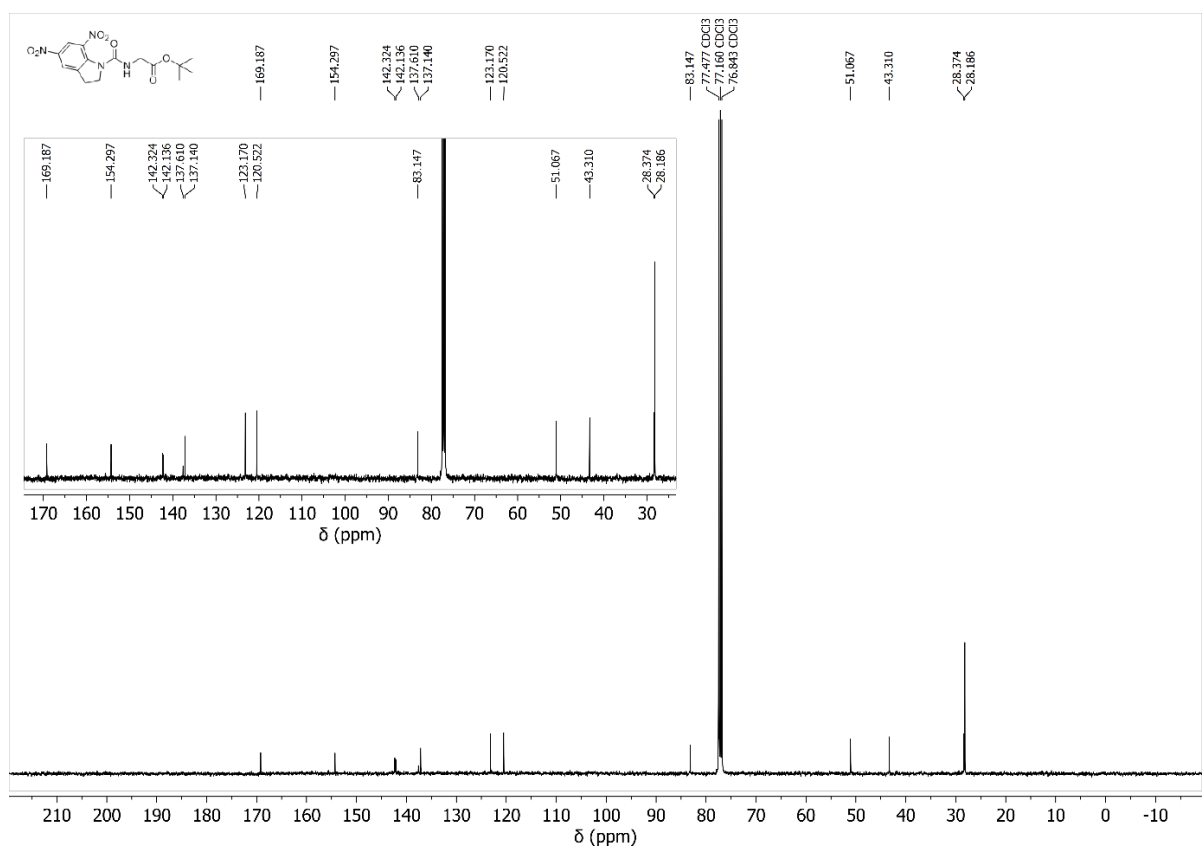


Figure S20: ¹³C NMR (101 MHz, CDCl₃) spectra of 6-tBu.

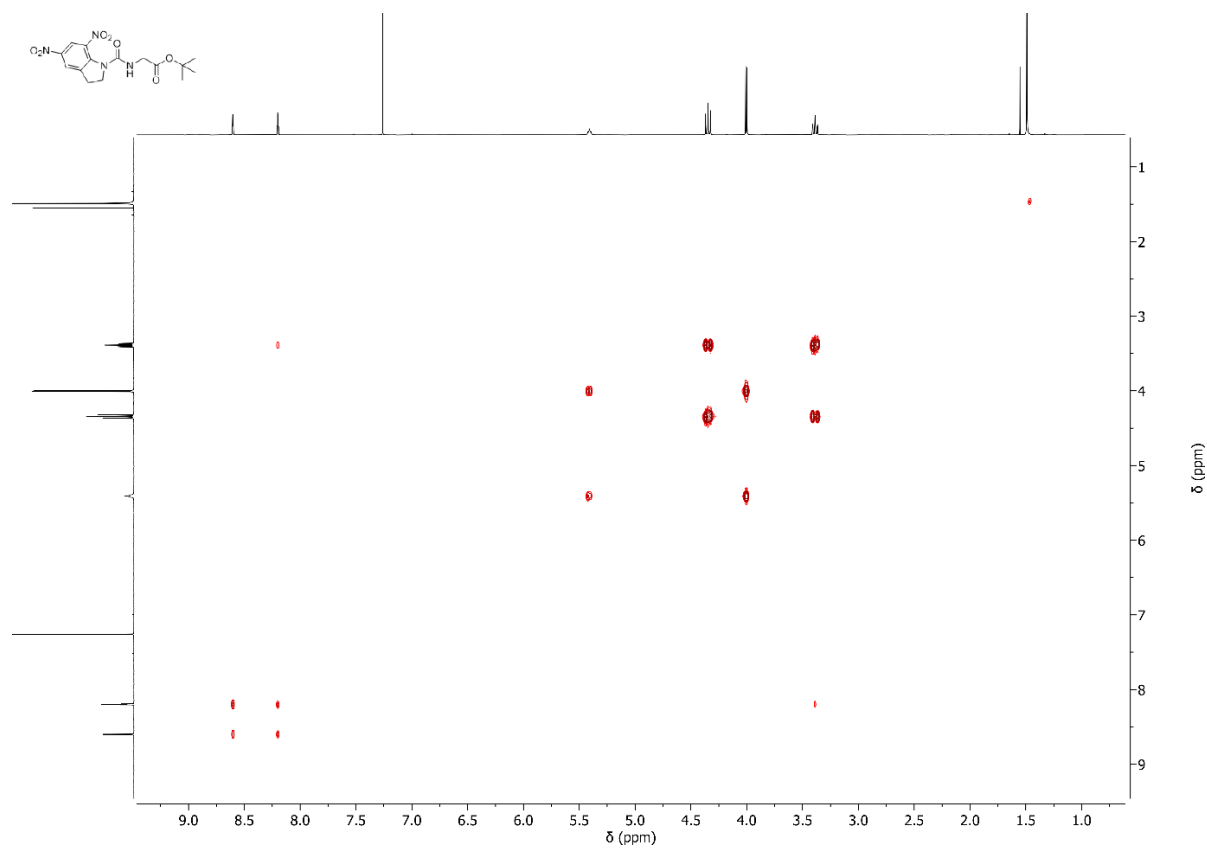


Figure S21: COSY NMR (CDCl₃) spectra of **6-tBu**.

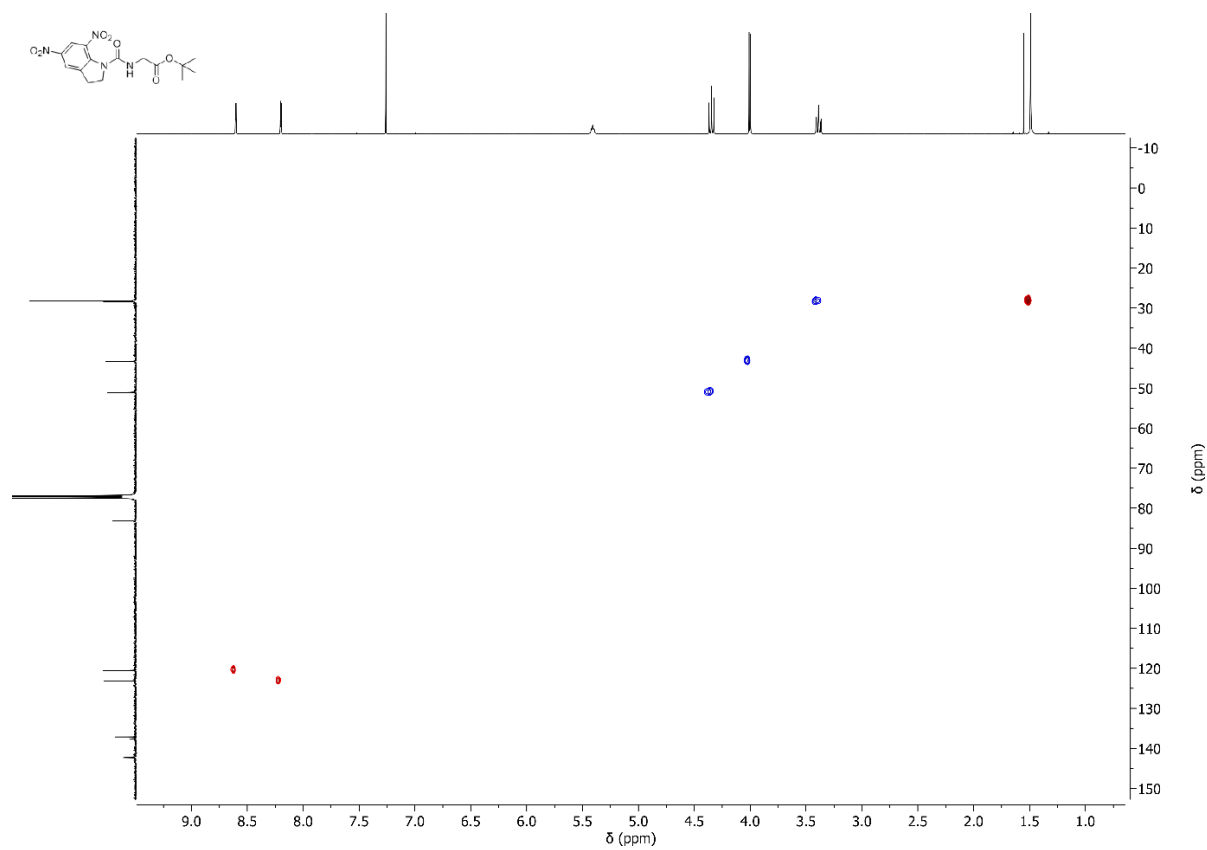


Figure S22: HSQC NMR (CDCl₃) spectra of **6-tBu**.

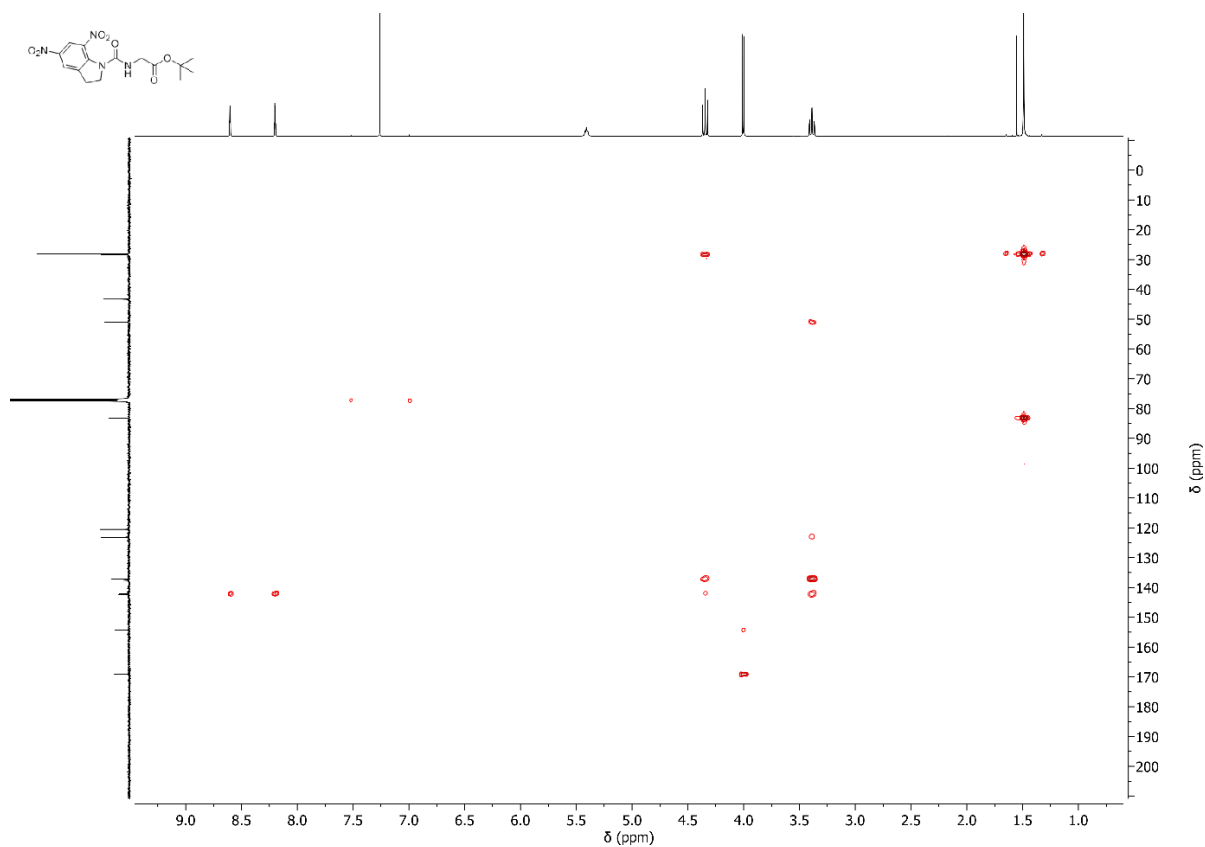


Figure S23: HMBC NMR (CDCl₃) spectra of 6-tBu.

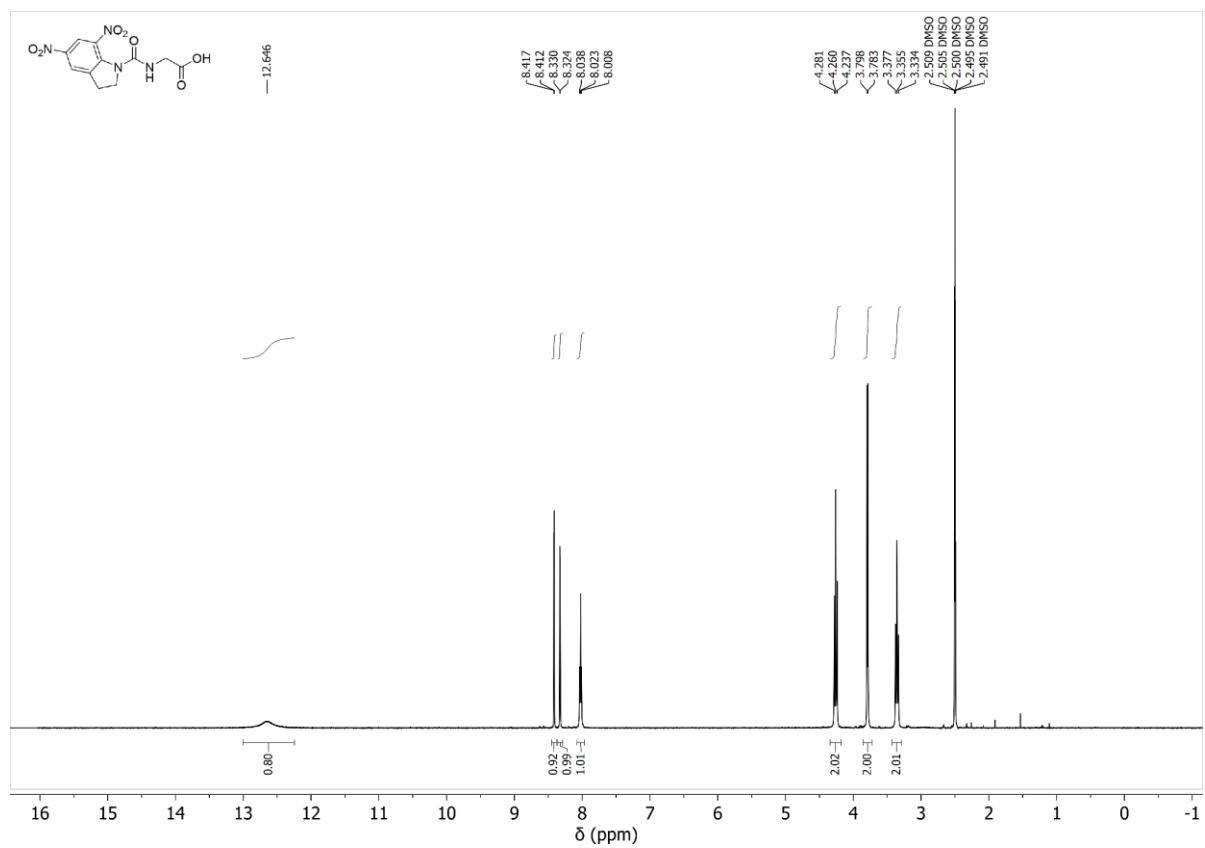


Figure S24: ¹H NMR (400 MHz, DMSO-d₆) spectra of 7-OH.

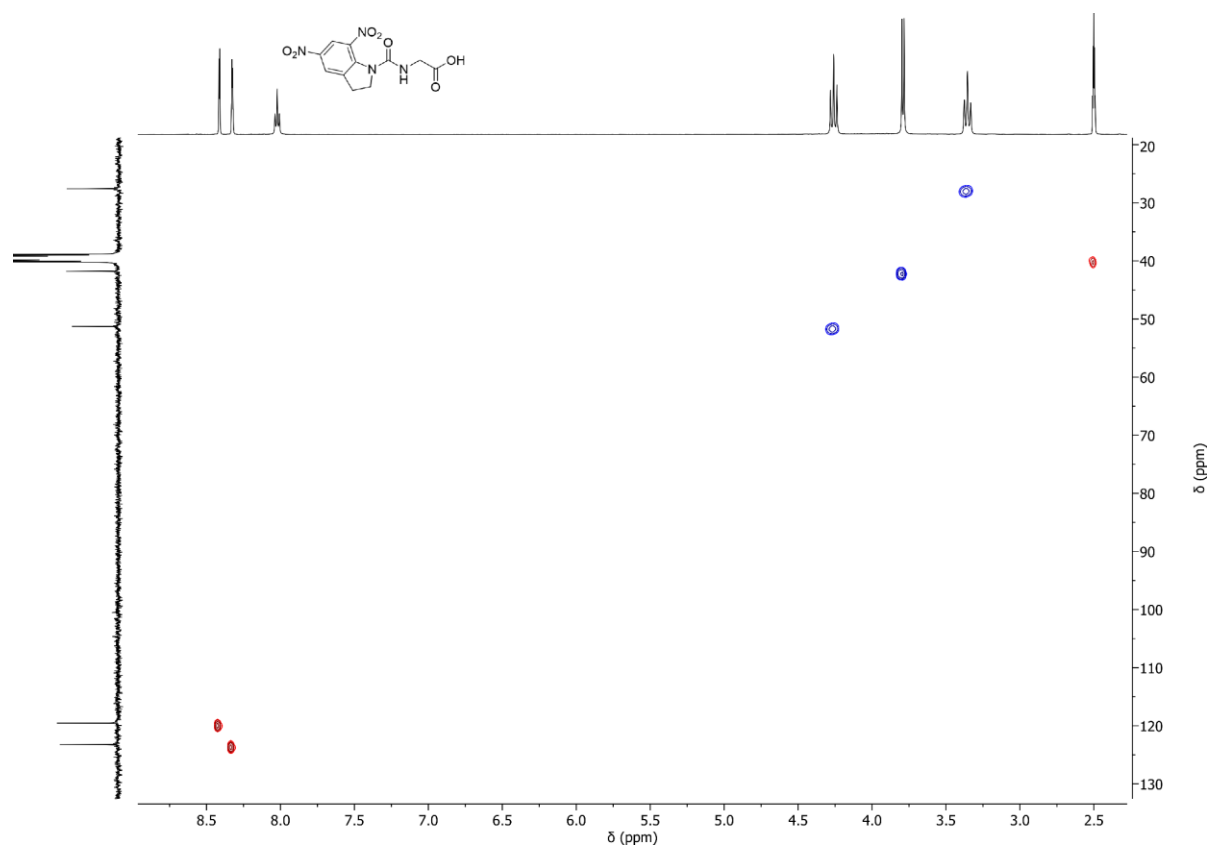


Figure S27: HSQC NMR (DMSO-d₆) spectra of 7-OH.

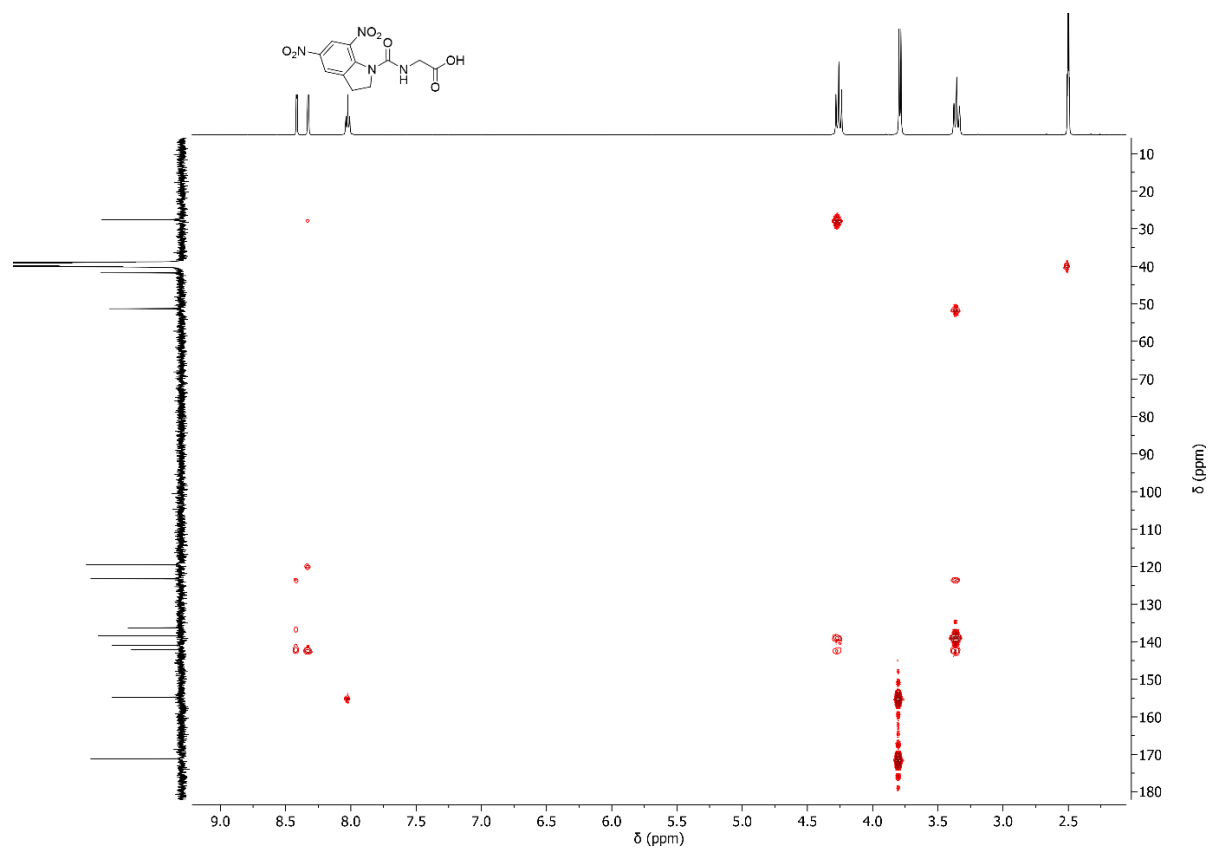


Figure S28: HMBC NMR (DMSO-d₆) spectra of 7-OH.

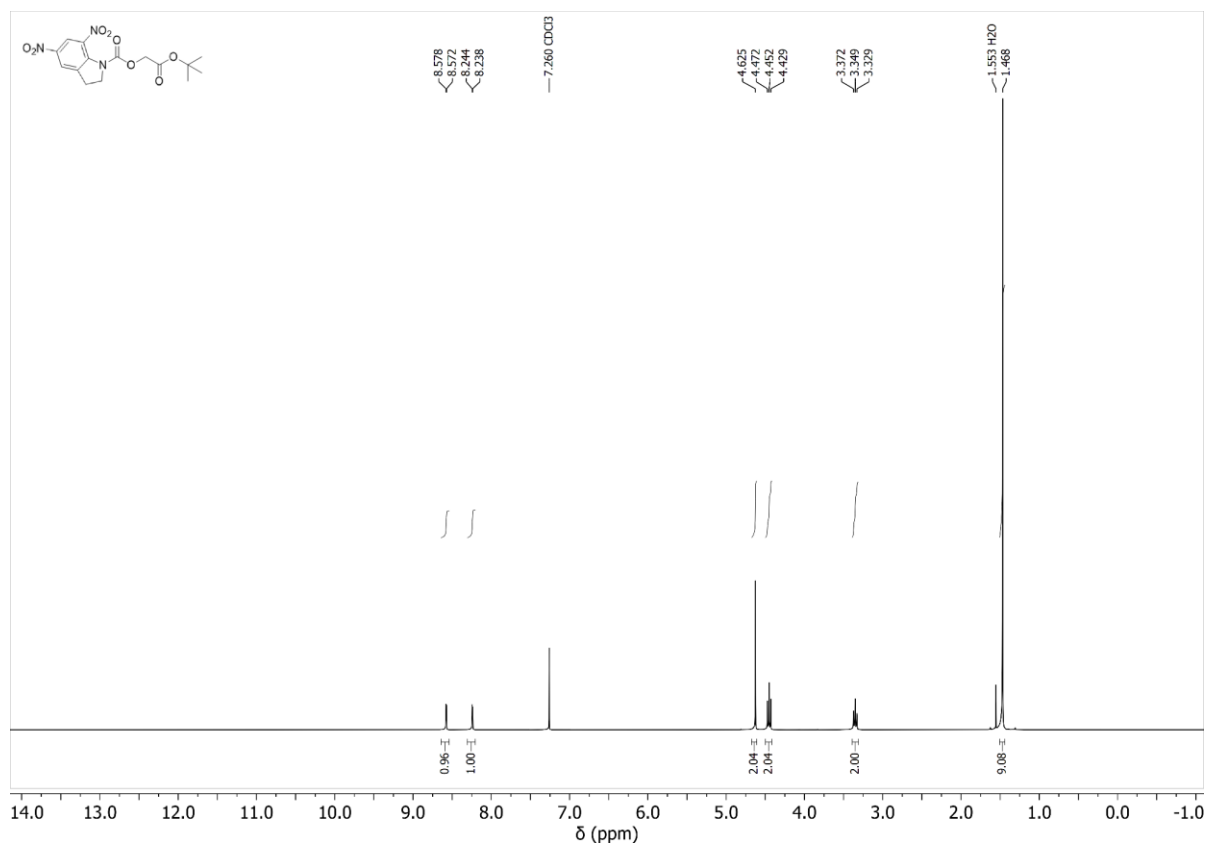


Figure S29: ¹H NMR (400 MHz, CDCl₃) spectra of 8-tBu.

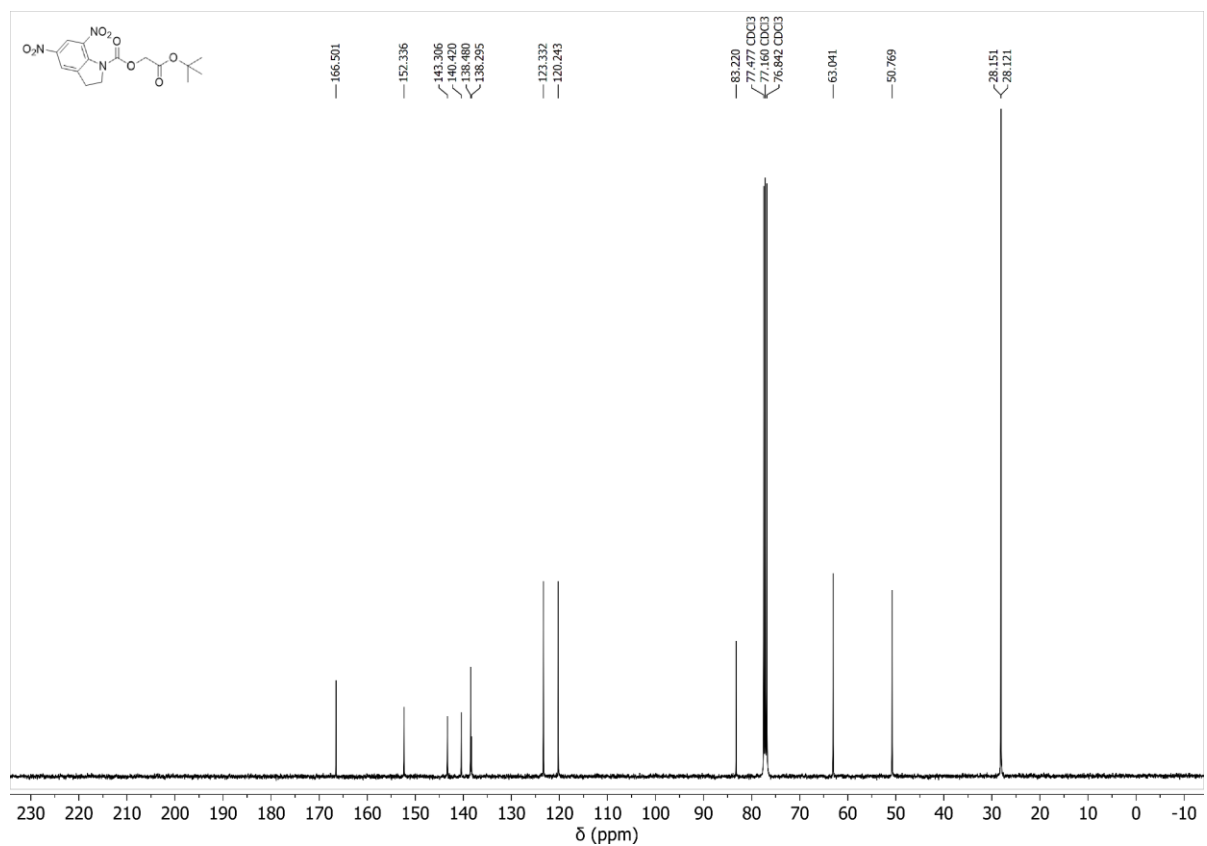


Figure S30: ¹³C NMR (101 MHz, DMSO-d₆) spectra of 8-tBu.

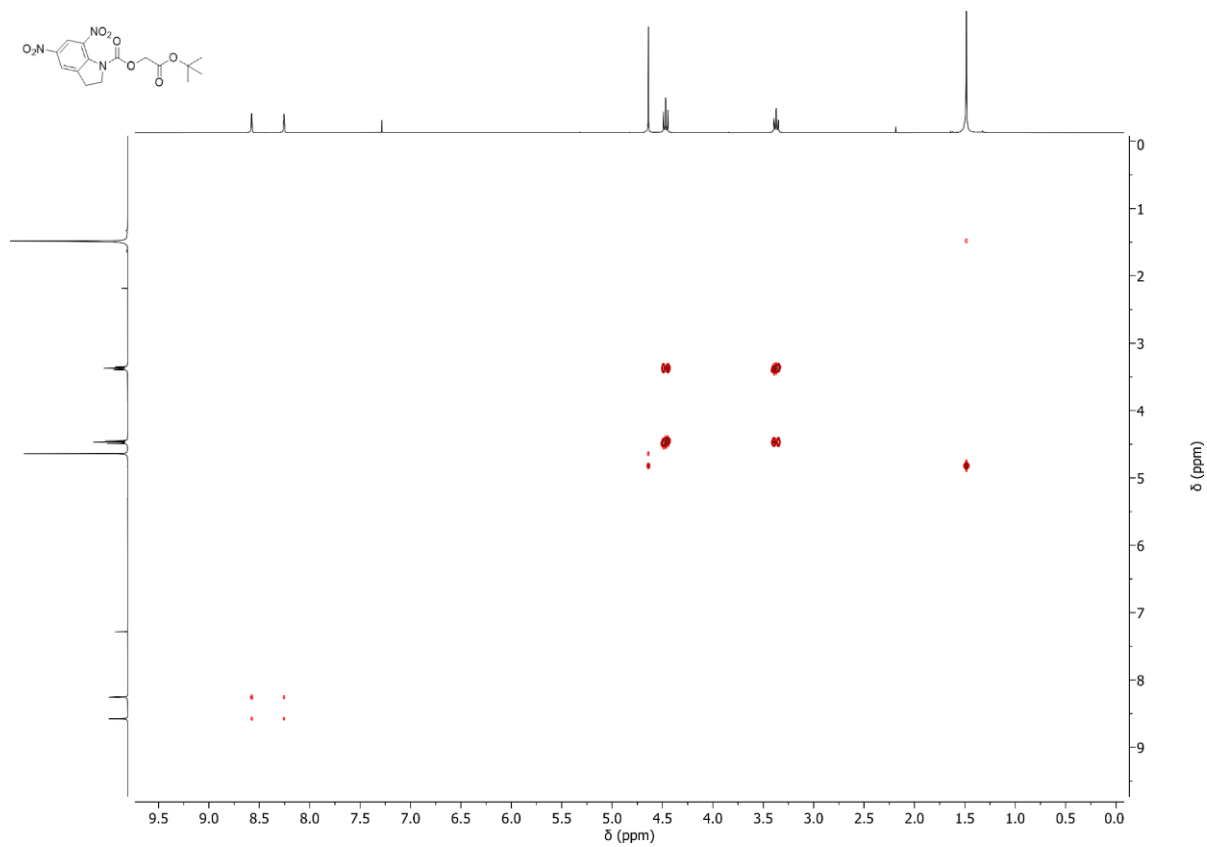


Figure S31: COSY (CDCl₃) spectra of **8-tBu**.

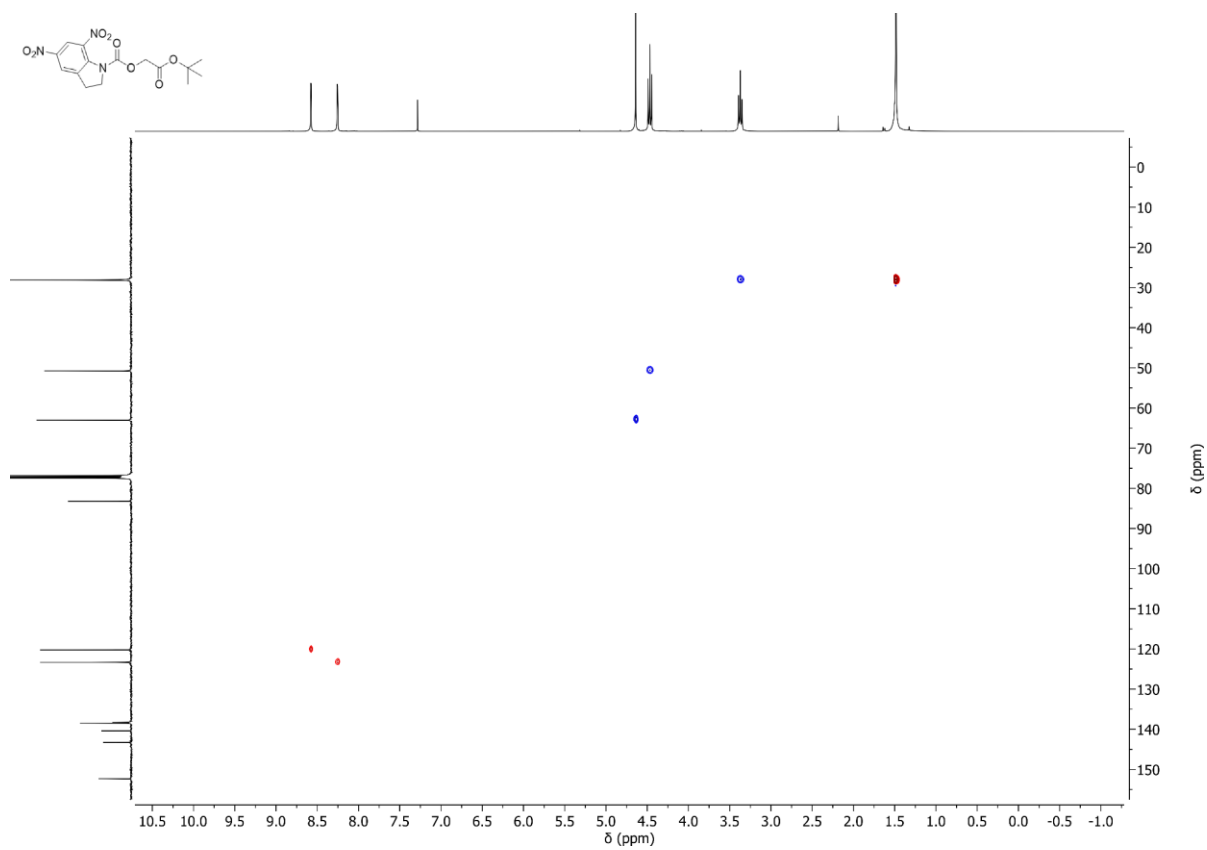


Figure S32: HSQC (CDCl₃) spectra of **8-tBu**.

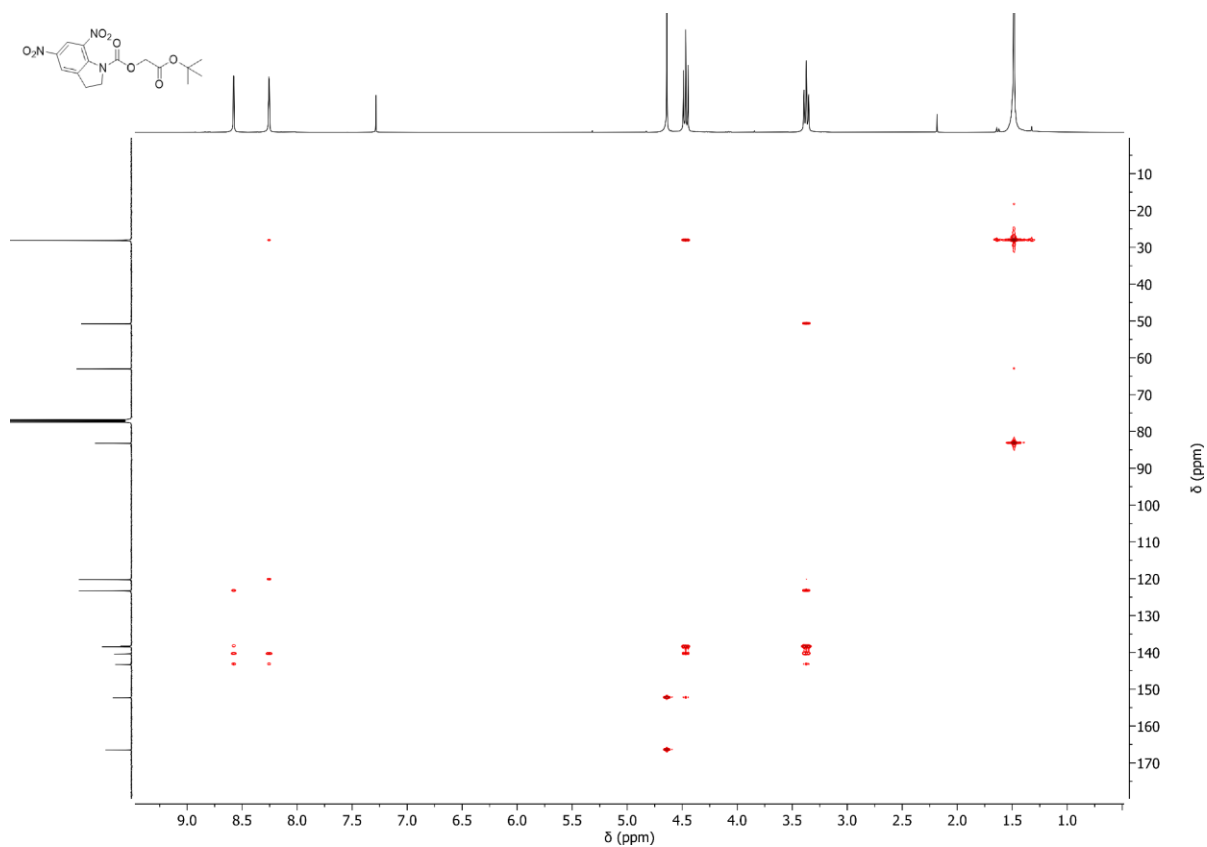


Figure S33: HMBC (CDCl₃) spectra of **8-tBu**.

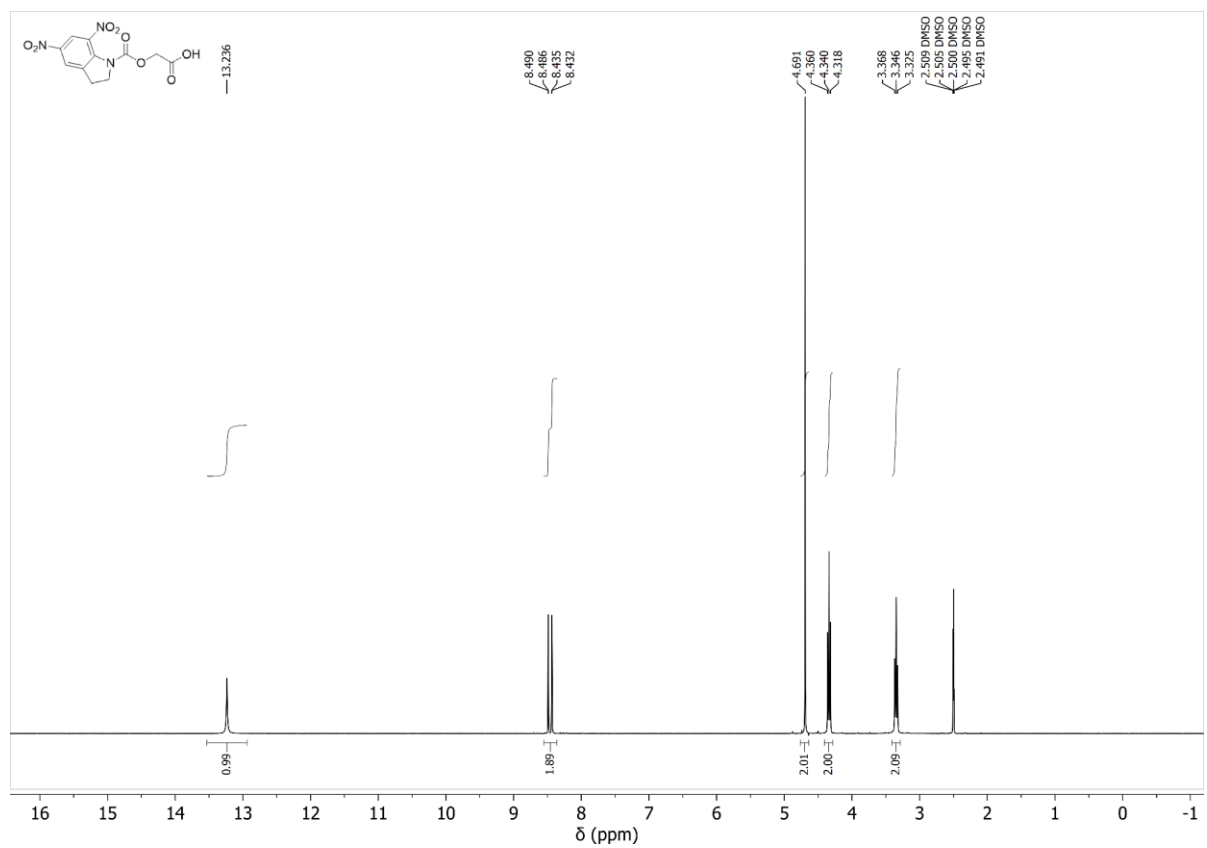


Figure S34: ¹H NMR (400 MHz, DMSO-d₆) spectra of **9-OH**.

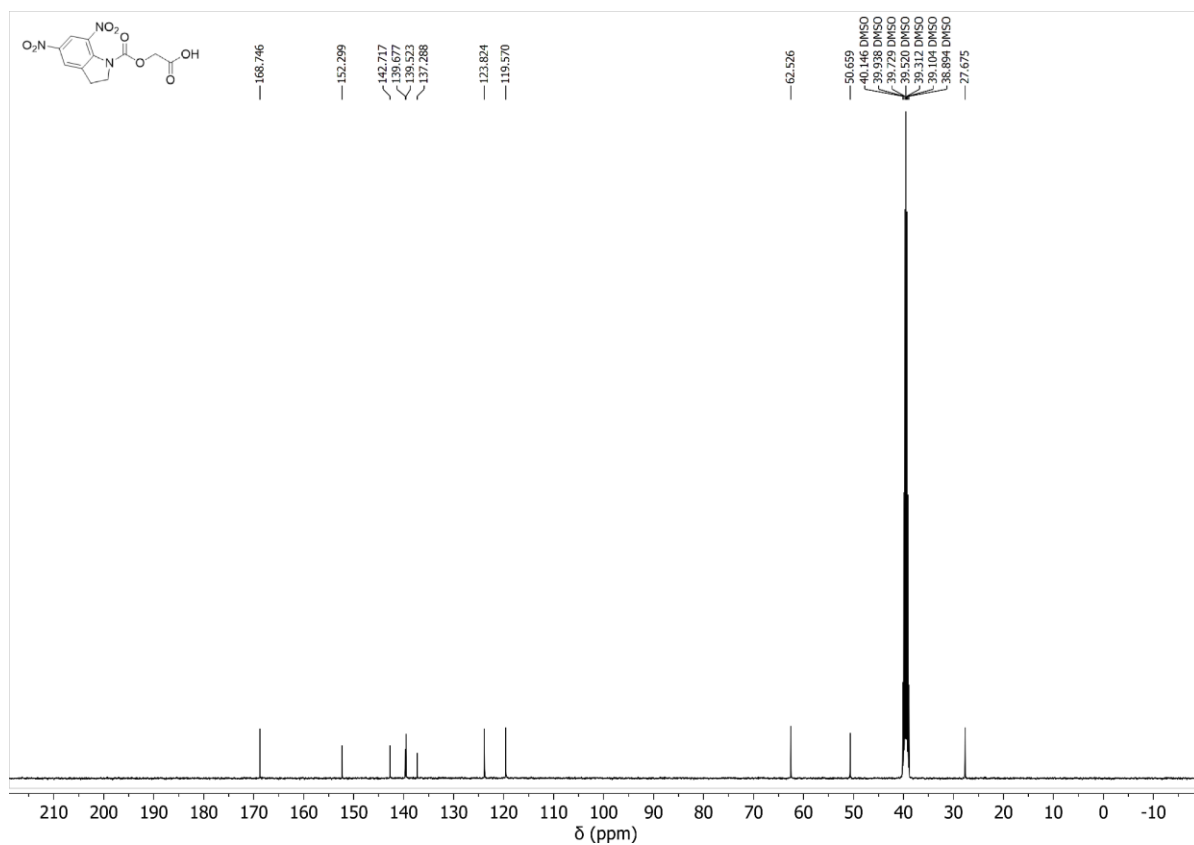


Figure S35: ^{13}C NMR (101 MHz, DMSO- d_6) spectra of 9-OH.

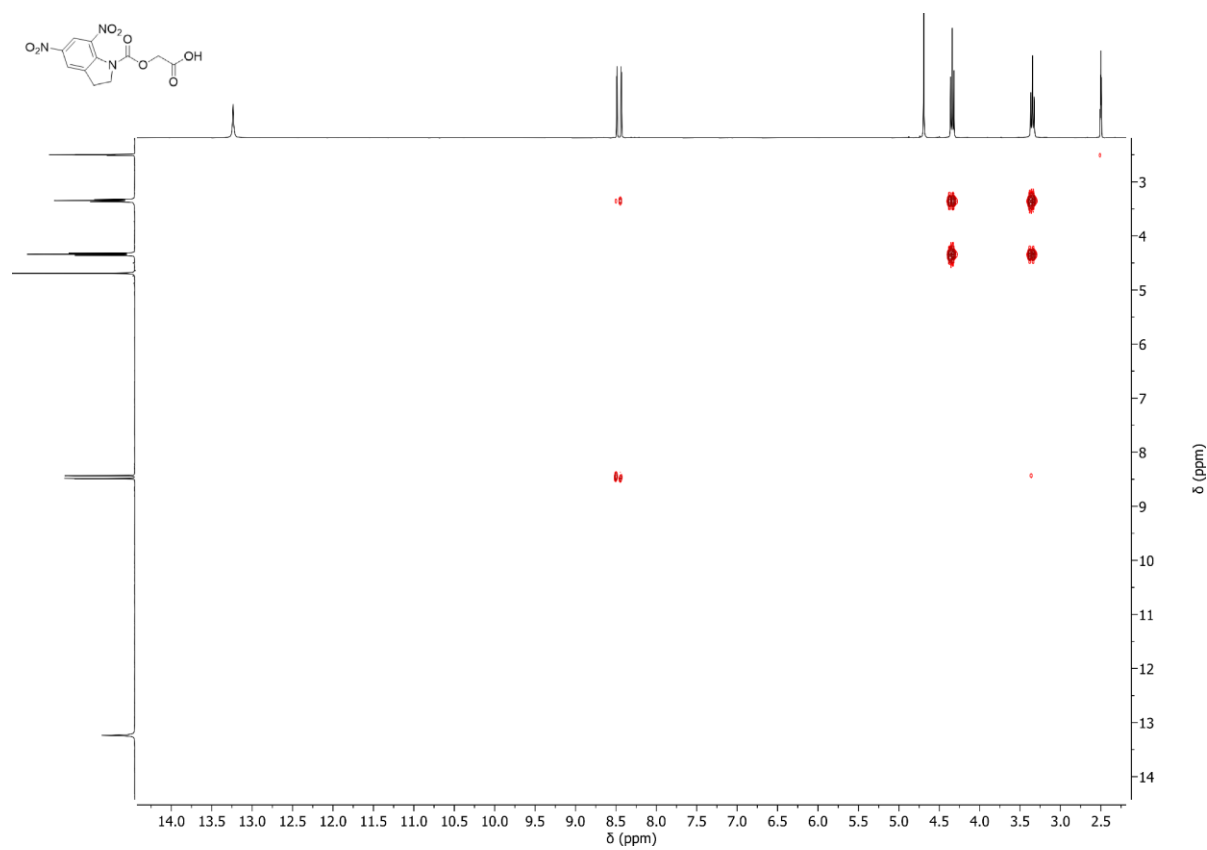


Figure S36: COSY NMR (DMSO- d_6) spectra of 9-OH.

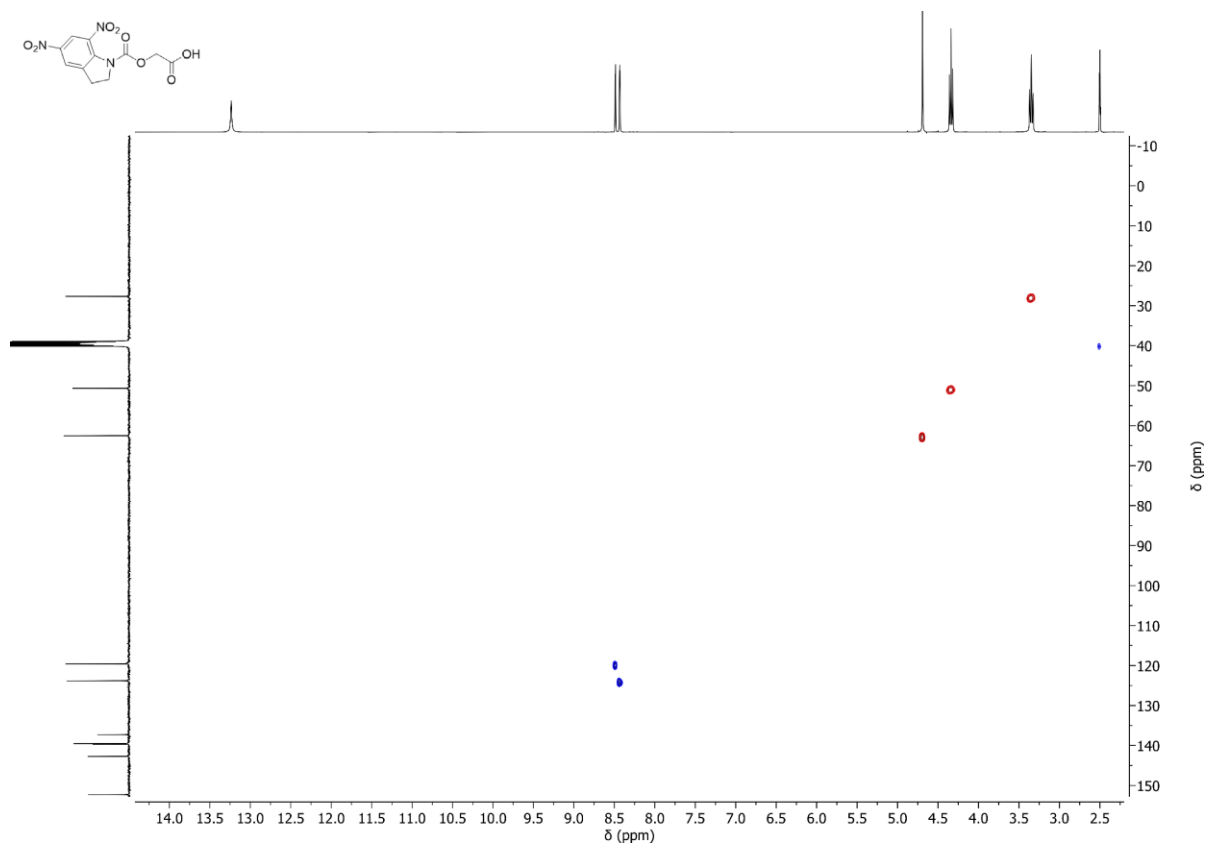


Figure S37: HSQC NMR (DMSO-d₆) spectra of **9-OH**.

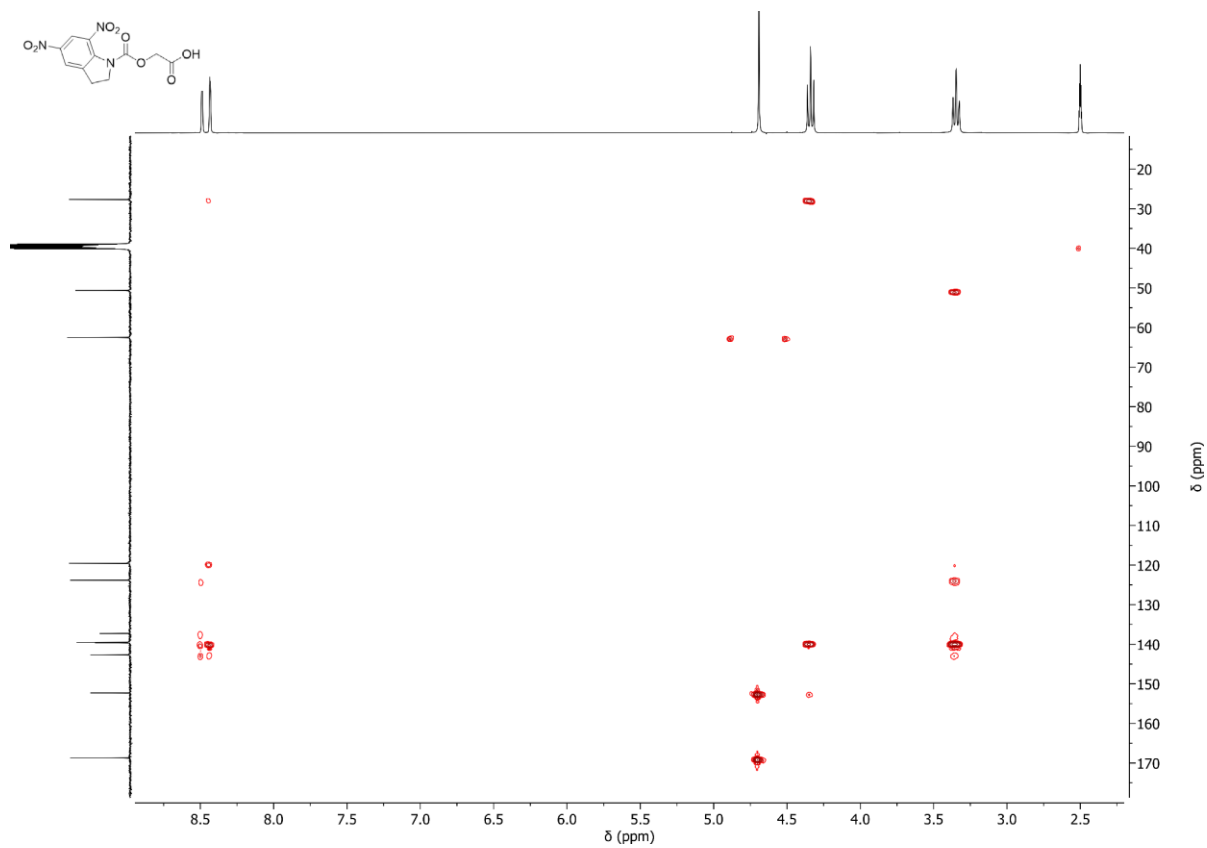


Figure S38: HMBC NMR (DMSO-d₆) spectra of **9-OH**.

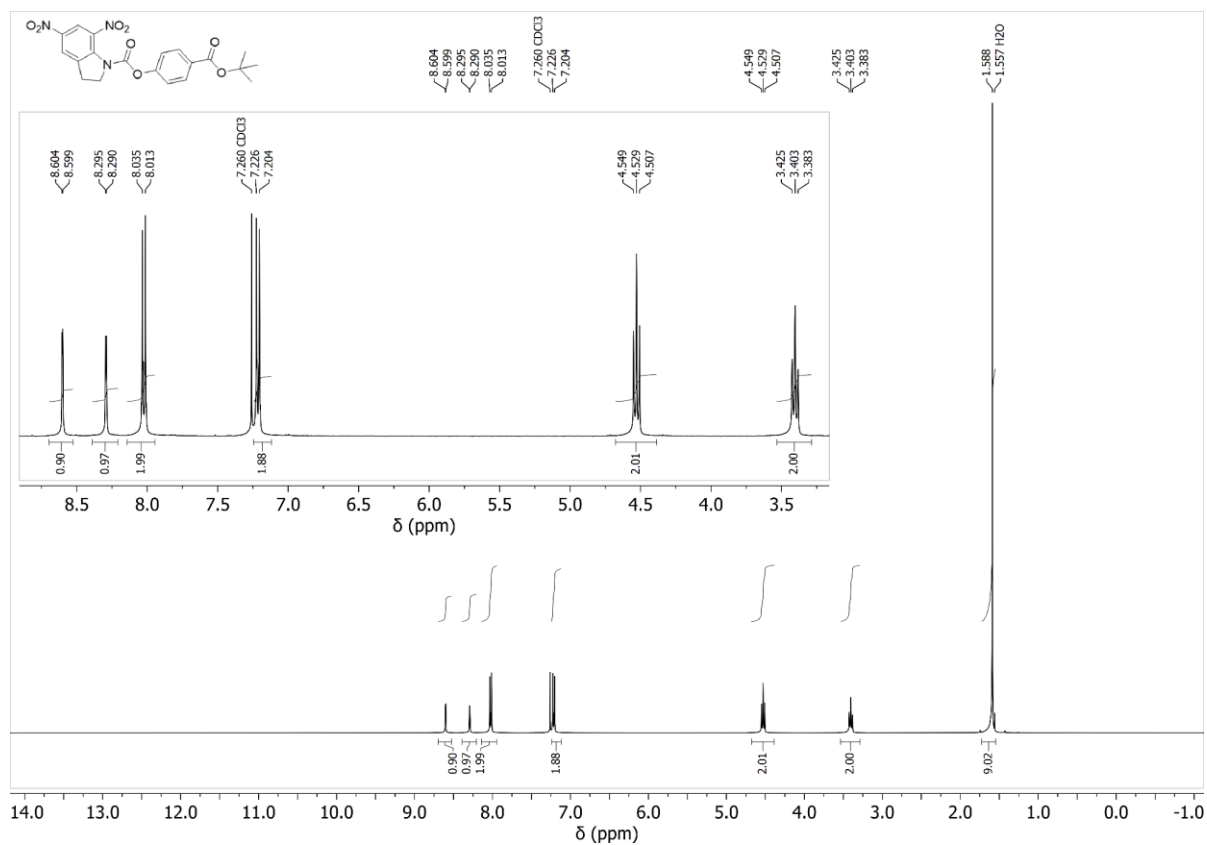


Figure S39: ¹H NMR (400 MHz, CDCl₃) spectra of 10-*t*Bu.

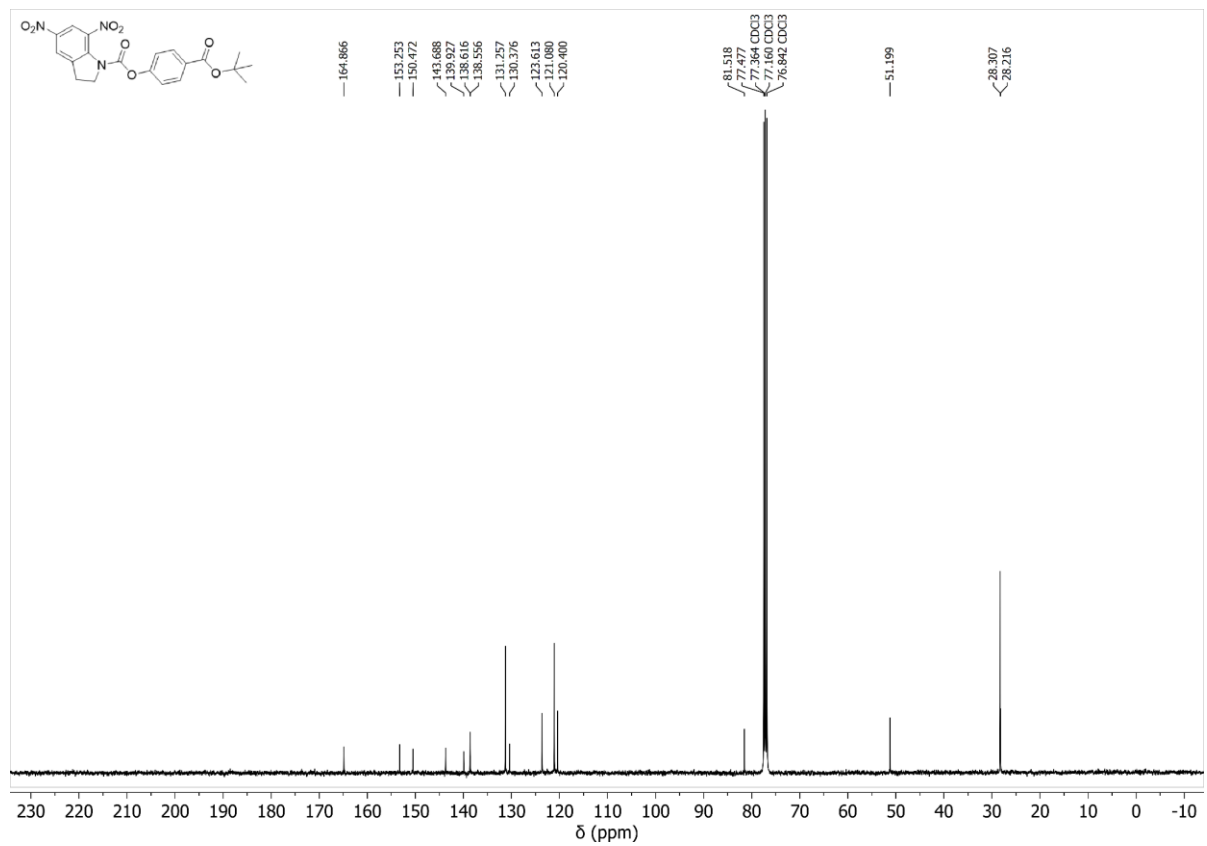


Figure S40: ¹³C NMR (101 MHz, CDCl₃) spectra of 10-*t*Bu.

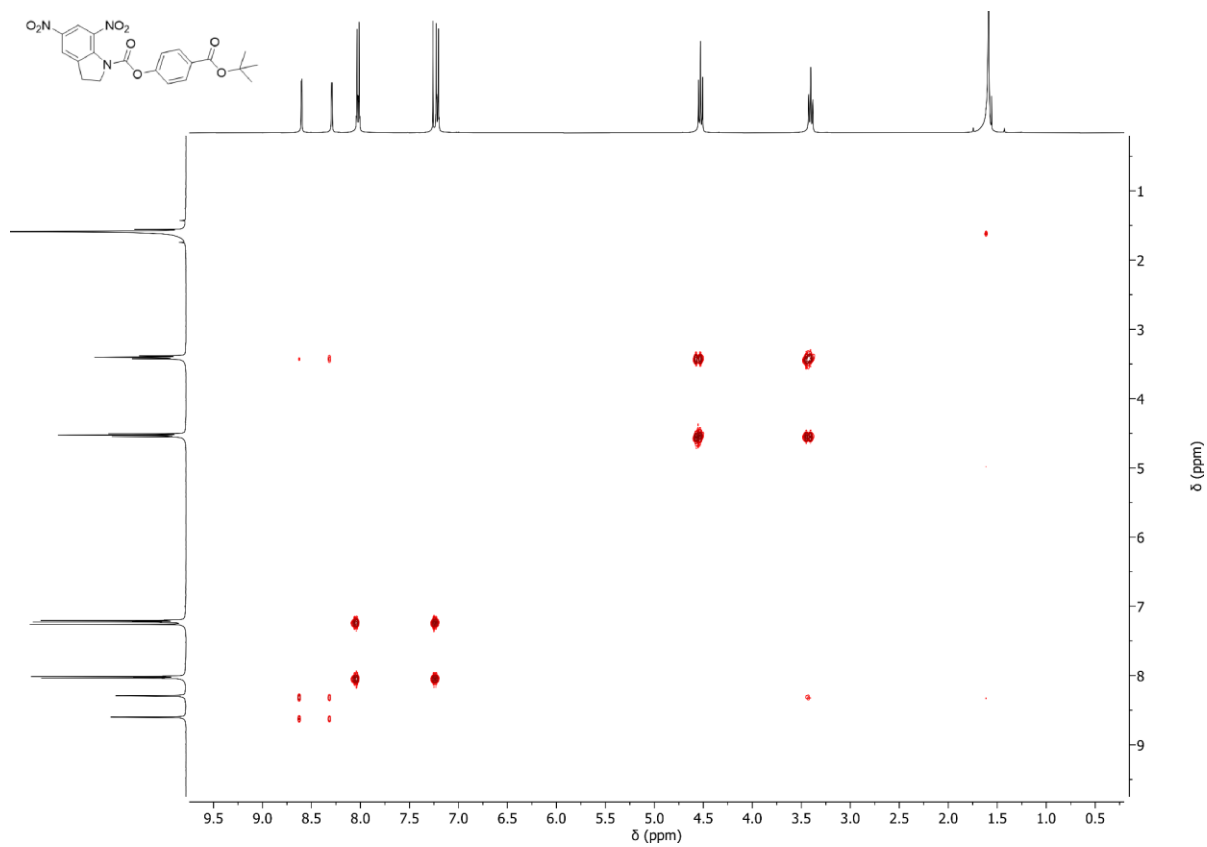


Figure S41: COSY NMR (CDCl_3) spectra of **10-tBu**.

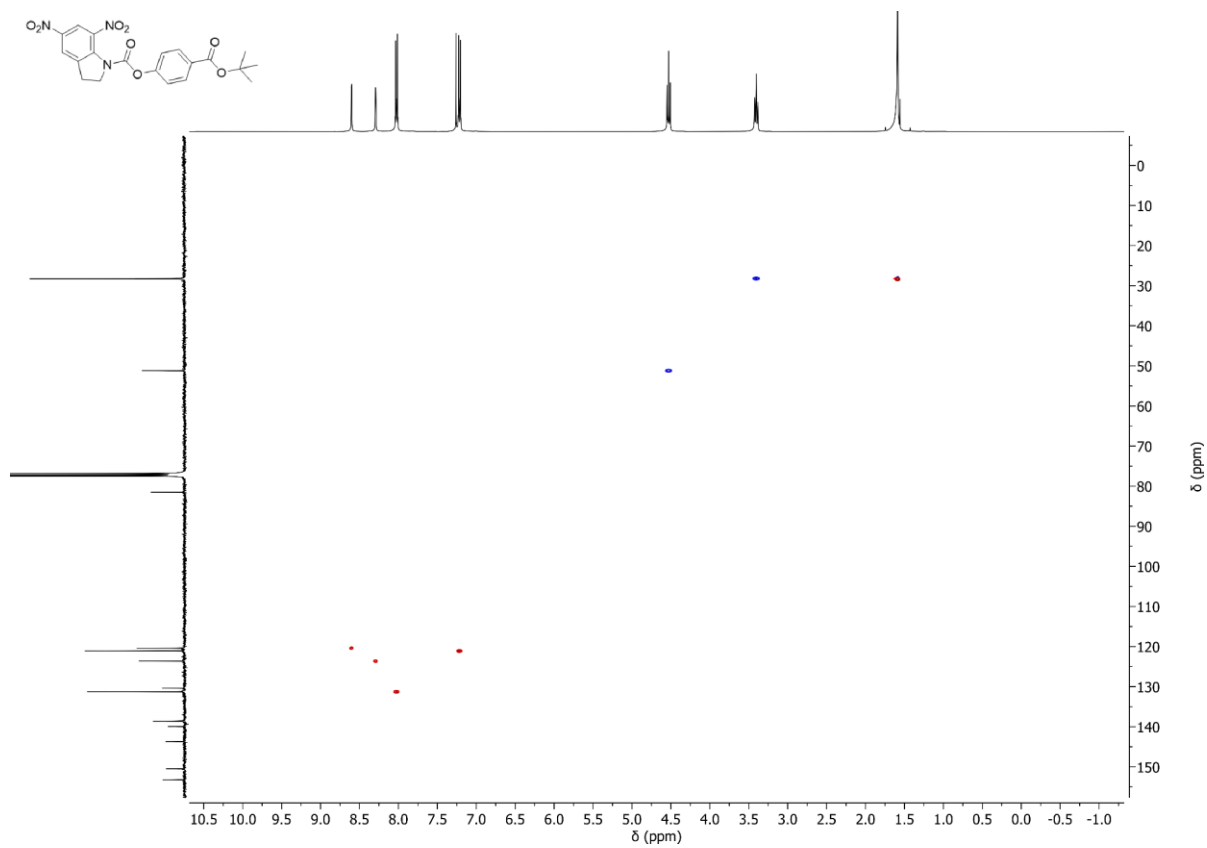


Figure S42: HSQC NMR (CDCl_3) spectra of **10-tBu**.

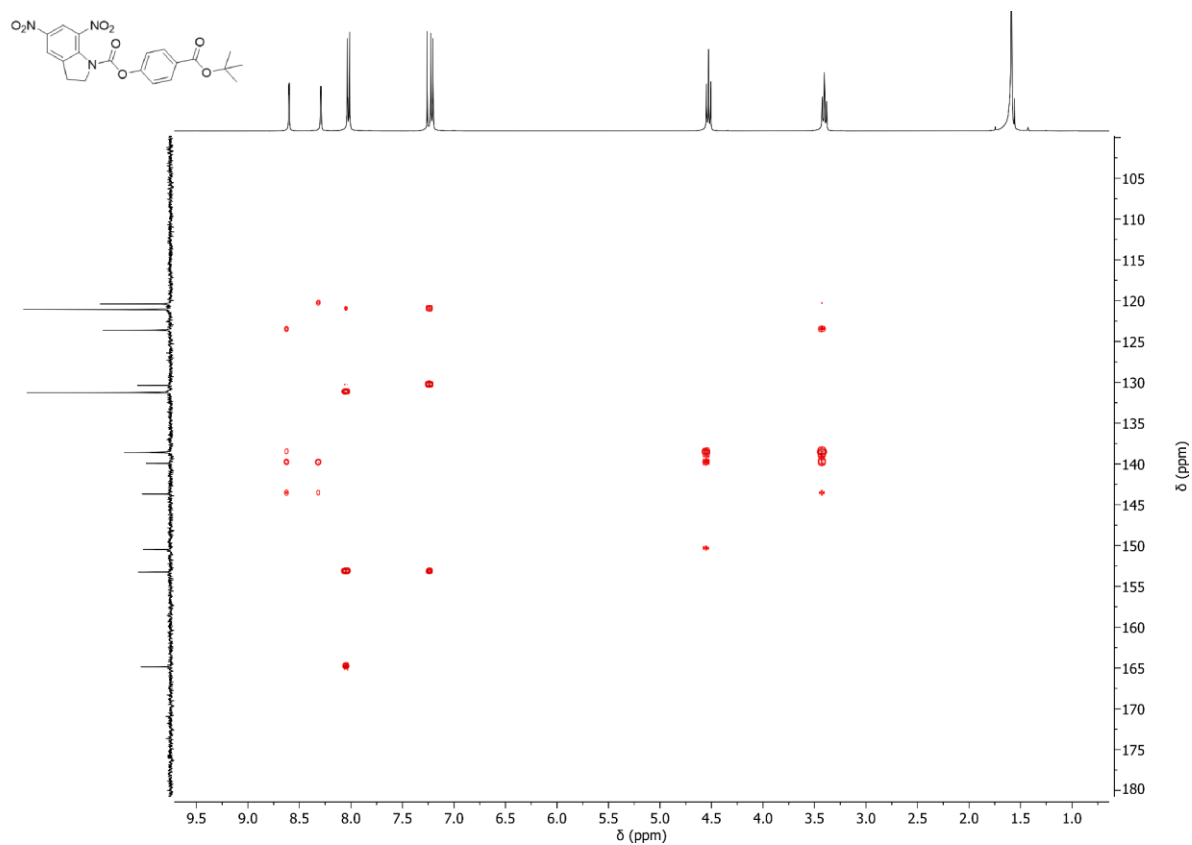


Figure S43: HMBC NMR (CDCl_3) spectra of 10-tBu.

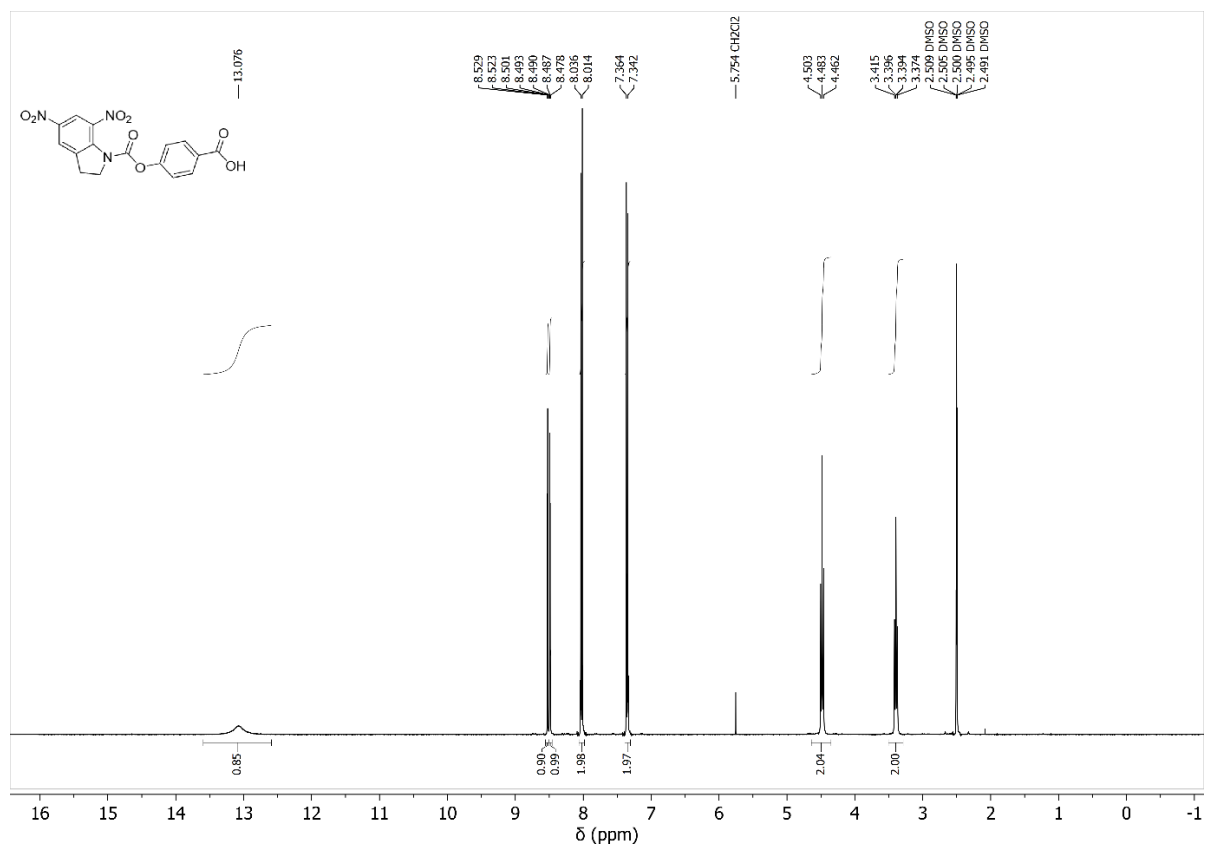


Figure S44: ^1H NMR (400 MHz, DMSO-d_6) spectra of 11-OH.

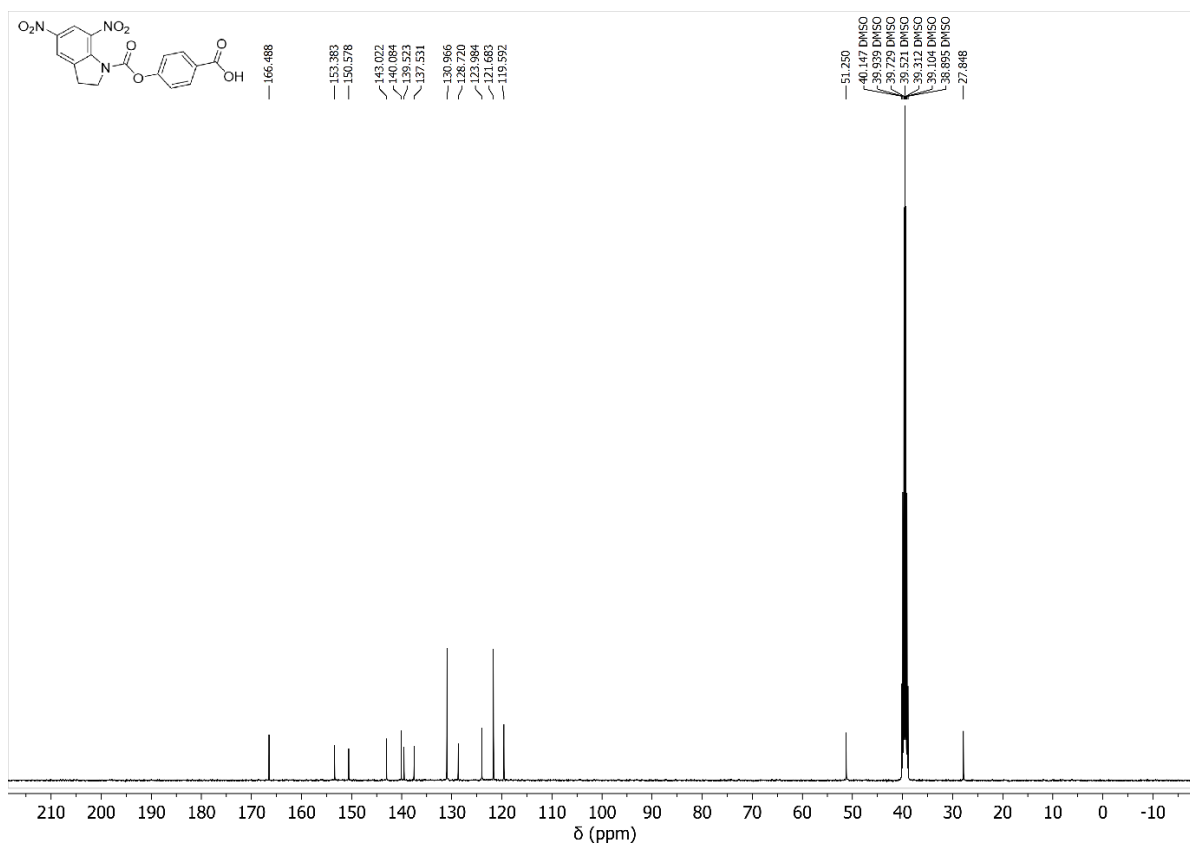


Figure S45: ^{13}C NMR (101 MHz, DMSO- d_6) spectra of **11-OH**.

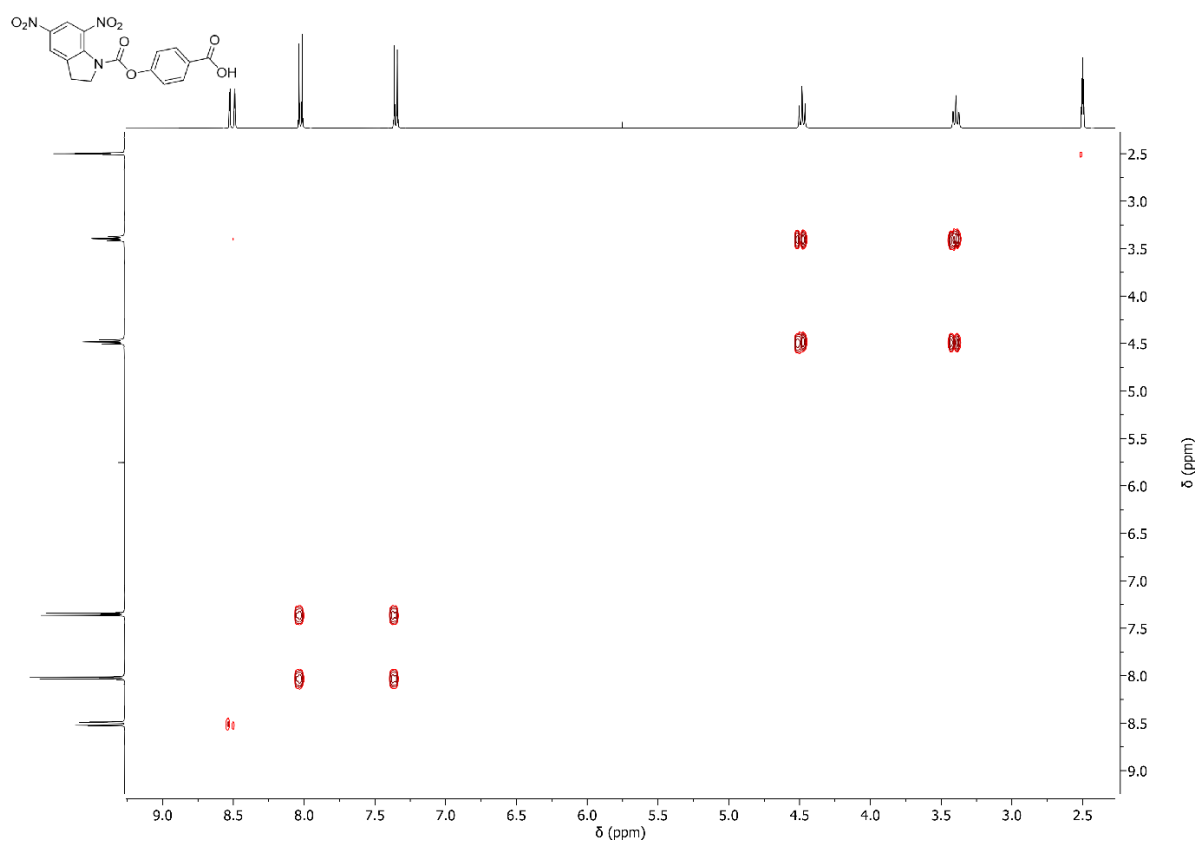


Figure S46: COSY NMR (DMSO- d_6) spectra of **11-OH**.

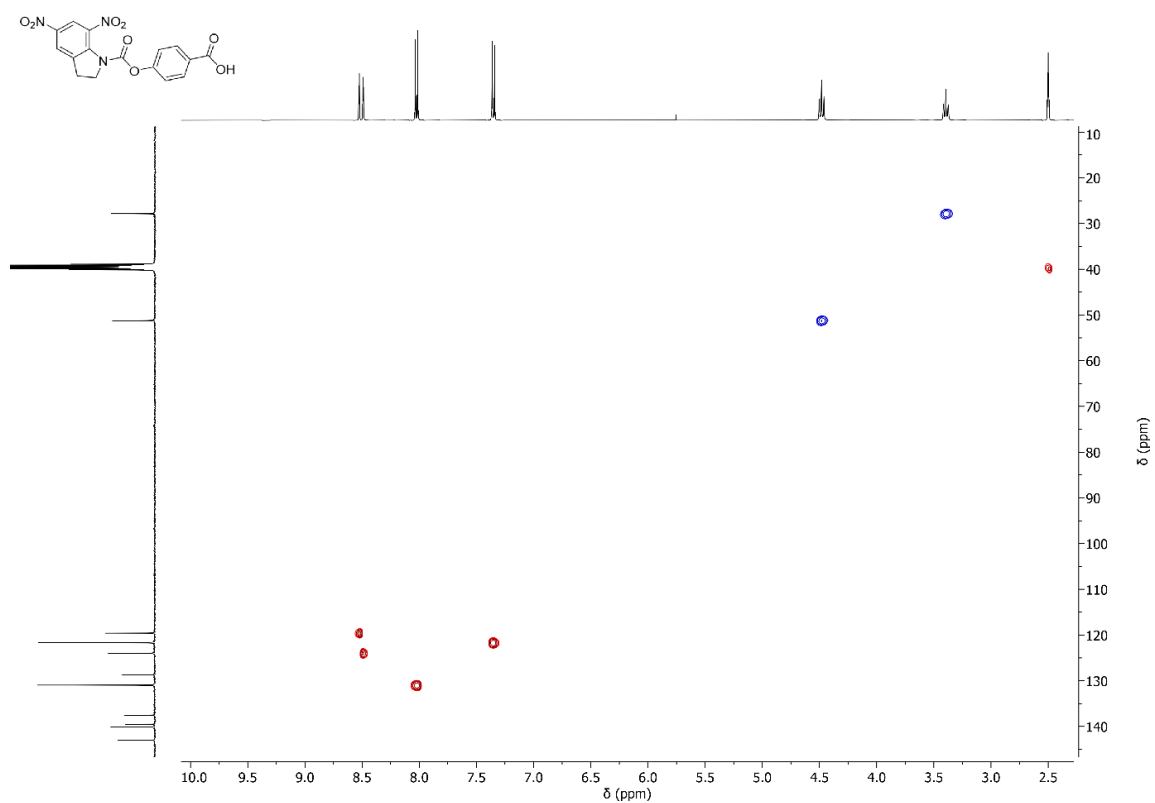


Figure S47: HSQC NMR (DMSO-d₆) spectra of **11-OH**.

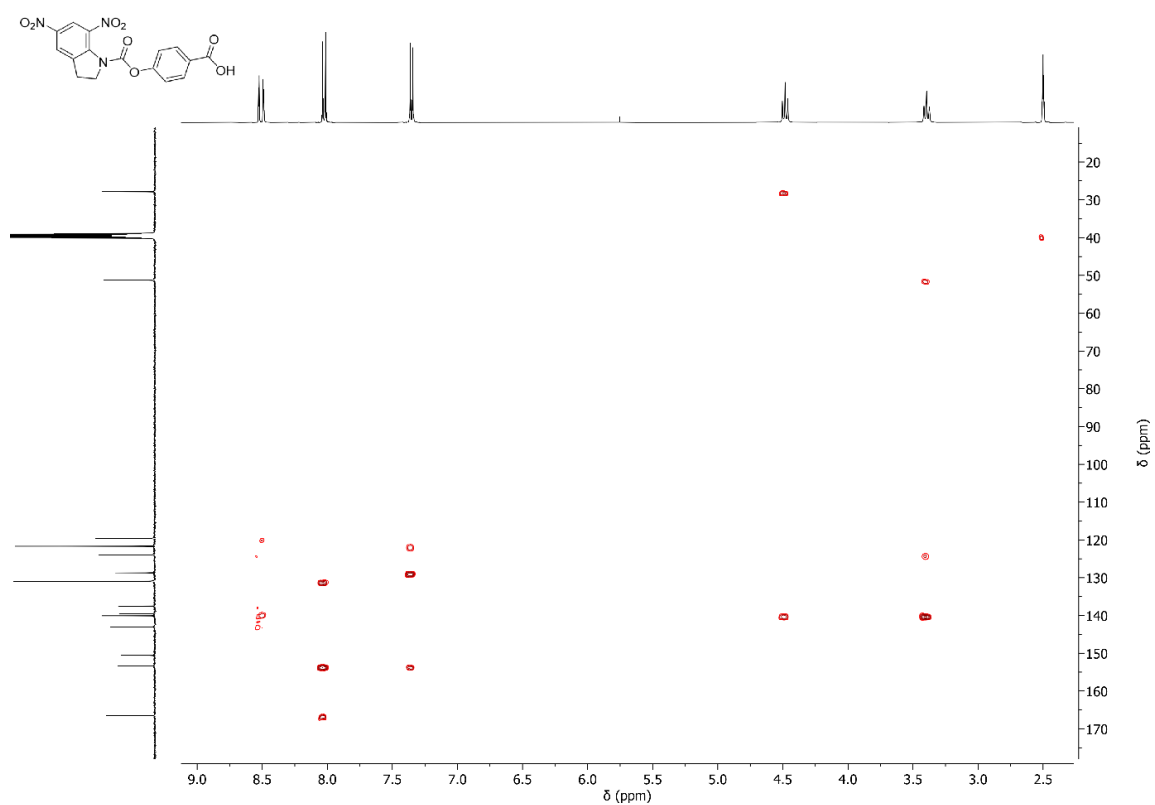


Figure S48: HMBC NMR (DMSO-d₆) spectra of **11-OH**.

References

- 1 A. Hassner, D. Yagudayev, T. Pradhan, A. Nudelman, B. Amit, *Synlett*, 2007, 2405–2409.